

# **A to Z of Terahertz Spectroscopy and 3D Sub-surface Imaging Experiments and other terahertz topics**

**Anis Rahman PhD**  
**Applied Research & Photonics**

<http://arphotonics.net>

Email: [info@arphotonics.net](mailto:info@arphotonics.net)

Phone: +1-(717) 623-8201

## **An eBook based on the following**

1. Tutorial presented at the Biosensors and Bioelectronics 2016, Phoenix, AZ, September 21 – 25, 2016
2. Invited talk presented at the [Semicon West 2018](#), Smart Manufacturing/Meet Experts Theater: Equipment Intelligence, Moscone South, San Francisco, CA July 10 – 12, 2018

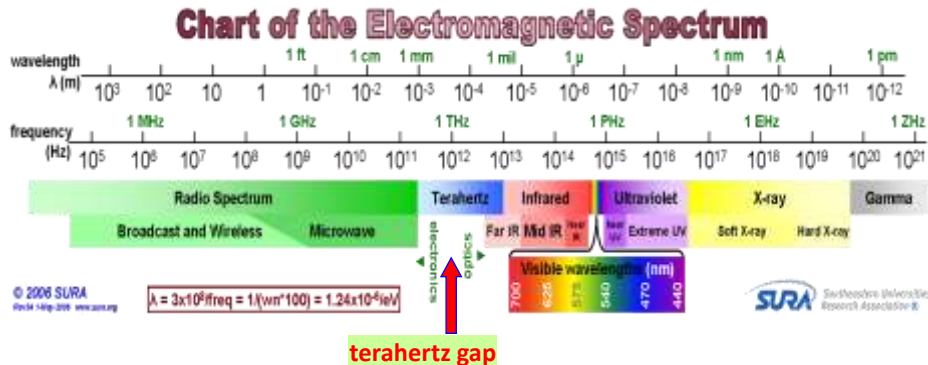
(C) 2018 Anis Rahman

## **Content**

- **What is terahertz?**
- **Why is it important?**
- **Integrated terahertz spectrometer/imager**
- **Sample considerations**
- **Measurements**
  - Spectral
  - 3D scanning
- **Spectra generation and analysis**
- **Image generation and analysis**
- **Practical examples**

(C) 2018 Anis Rahman

# What is terahertz?



- Raman/IR covers  $\sim 250$  to  $4000 \text{ cm}^{-1}$  → Bond, torsion
- THz covers  $0.1 \text{ THz}$  to  $\sim 30 \text{ THz}$  (from  $\sim 3$  to  $1200 \text{ cm}^{-1}$ )
- All kinds of molecular resonances, Molecular backbone, intermolecular interaction
- Non-ionizing → soft tissue

(C) 2018 Anis Rahman

3

## Why Terahertz?

- Non-ionizing, can penetrate
- Deploying Terahertz for high sensitivity spectroscopy
- Non-destructive, non-contact inspection on and under the surface
- Multispectral imaging with  $<1 \text{ nm}$  resolution
- Layer-by-layer imaging and spectral analysis
- Characterize 0D -- 3D nanomaterials
- Semiconductor defect analysis
- Early detection of skin cancer and health monitoring of soft tissues

(C) 2018 Anis Rahman

# Terahertz generation

Technology	Advantages	Challenges
Photo-conductor	<ul style="list-style-type: none"> <li>• Legacy technology</li> </ul>	<ul style="list-style-type: none"> <li>• Low output power, <math>\sim\mu\text{W}</math></li> <li>• High voltage &amp; pulsed laser</li> <li>• Limited THz range</li> </ul>
Difference Frequency Gen. (DFG)	<ul style="list-style-type: none"> <li>• Tunable, Pulsed or CW</li> <li>• Higher power (<math>\sim\text{mW}</math>)</li> <li>• Broadband or narrow</li> </ul>	<ul style="list-style-type: none"> <li>• Two lasers needed</li> <li>• Difficult alignment</li> <li>• Needs high <math>\chi^{(2)}</math> material</li> </ul>
<b>Dendrimer dipole excitation (DDE) <math>\rightarrow</math> ARP</b>	<ul style="list-style-type: none"> <li>• <b>No pulsed laser, no high voltage, compact</b></li> <li>• <b>Tunable output power &amp; range</b></li> </ul>	<ul style="list-style-type: none"> <li>• <b>New technology</b></li> <li>• <b>Dendrimer doping and poling</b></li> </ul>
Reactor Synchrotron	<ul style="list-style-type: none"> <li>• Higher output power</li> </ul>	<ul style="list-style-type: none"> <li>• Huge in size and cost</li> <li>• Limited THz range</li> <li>• Needs dedicated facility</li> </ul>
QCL	<ul style="list-style-type: none"> <li>• No pump laser</li> </ul>	<ul style="list-style-type: none"> <li>• Unstable, fixed bandwidth, low power, not tunable, fab, low temp.</li> </ul>

(C) 2018 Anis Rahman



ARP Team with **Robert F. Curl, Jr.**, (NL, Chemistry 1996) & **Sir Harold Kroto** (NL, Chemistry 1996),

**“Everyone knows that better THz sources are important to scientific progress...”**  
**-Robert F. Curl, Jr.**

## Terahertz generation by Dendrimer Dipole Excitation

- $W_{THz} \propto \chi^{(2)} W_{pump}^2$
- THz power  $\uparrow$  as  $\chi^{(2)} \uparrow$
- $\chi^{(2)} = nf\beta \langle \cos^3 \theta \rangle$

$n$  dipole density

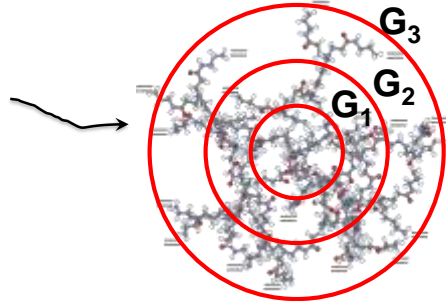
$f$  local field factor

$\beta$  average hyperpolarizability

$\theta$  dipole alignment angle

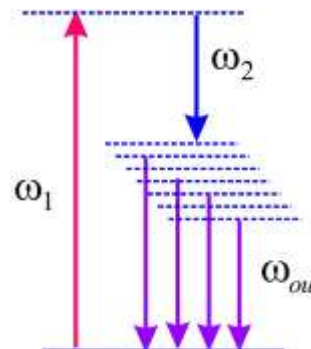
$$\Rightarrow \mu(x) = ql(x)$$

- Unlike inorganics, dendrimer offers a distribution of charge centers;  $l \rightarrow l(x)$
- There are many chromophores to choose from  $\rightarrow$  tunability

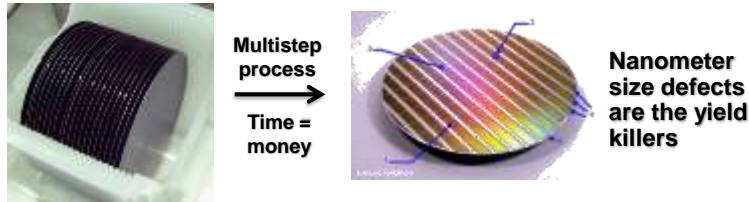


## Dendrimer Dipole Excitation (DDE)

- Energy level diagram of dendrimer resulting from chromophore doping and poling
- A distribution of dipole moments creates CW broadband emission via DDE when pumped by a suitable laser.
- No separate dispersion element needed
- Multispectral imaging



## A real world problem



- Assume 65 nm technology node: each die is 2.130 mm × 2.130 mm
- A single 8" wafer produces ~10000 chips (excluding kerf loss)
- E.g., ~10,000 CPU → \$100/CPU → **\$1M**
- Blank wafer ~\$100/piece → 10,000X value increase!
- Undetected defect lowers the yield → **Big problem**
- <1 nm size defect must be detected for 10 nm node
- Current (destructive) techniques take very long to arrive finished product
- Smart, 3D, non-destructive, nano-scale metrology is needed

(C) 2018 Anis Rahman



## Current solutions are not adequate

- Semiconductor manufacturers need “<1 nm resolution” imaging capability
- Also need: sub-nanometer, sub-surface, non-contact, non-destructive, 3D inspection
- Current art: Optical, X-Ray, Atomic Force Microscopy, SEM, TEM, Focused Ion Beam, etc. all suffer from limitations
  - Customers often perform multiple measurements
  - Expensive and destructive
  - Multiple instrument/analysis is required

(C) 2018 Anis Rahman



# Nanometrology

By nanometrology, we mean the measurement of any nano-scale things such as nanomaterials, nanoparticles, nanometer, nanosecond, etc. As the old saying goes, “If you can’t measure it, you can’t manage it.” So, the measurement is the key for any field.

**Challenge: Sub-nanometer resolution imaging without electron microscope, atomic force microscope, scanning tunneling microscope, focused ion beam, etc.**

## Introduction: Abbe diffraction limit

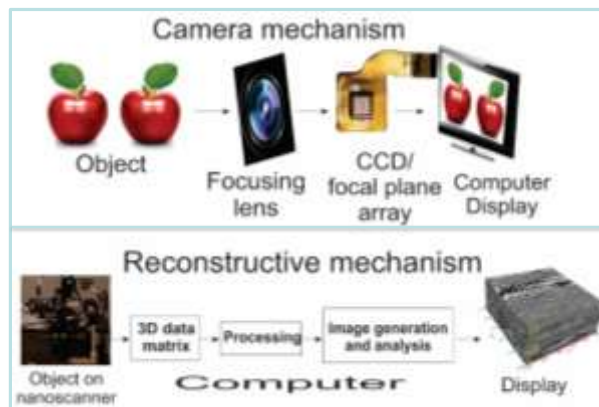
- The resolution  $d$  of an optical-lens-based imaging system is defined by the Abbe diffraction limit (“ADL”) [1];  $d = \frac{\lambda}{2n \sin \theta}$ , where  $\lambda$  is the wavelength. For free-space  $d \approx \lambda/2$ .
- Wavelength of electrons is much smaller than that of photons (2.5 pm at 200 keV)  $\rightarrow$  the resolution of an electron microscope (EM) is theoretically  $\sim 1.3$  pm. In practice, the resolution of an EM is limited to  $\sim 0.1$  nm due to the objective lens system.
- Current techniques, such as SEM, TEM, AFM, STM, and FIB produce a frozen-in-time image of a single surface.
- They are destructive and suitable for small sample sizes. Requires high vacuum and rigorous sample preparation.
- Q: how to break the Abbe diffraction limit?

[1] Ernest Abbe, Arch. Mikrosk. Anat. 9, 413 (1873)

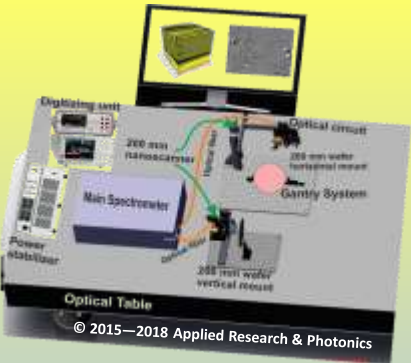
## Is Breaking ADL Enough?

- Breaking the ADL is required but NOT sufficient!
- For terahertz radiation (T-ray), the wavelengths are much bigger,  $\sim 9 \mu\text{m} < \lambda < 3 \text{mm}$ ! i.e.,  $0.1 \text{THz} < f < \sim 33 \text{THz}$ .
- Consequently, a resolution of less than  $4.5 \mu\text{m}$  breaks the ADL.
- But this does not help achieving  $< 1 \text{nm}$  resolution
- $\rightarrow$  *breaking the ADL is “required” but NOT “sufficient!”*
- Q: How to achieve  $< 1 \text{nm}$  image resolution?
- Here, a stratagem has been worked out that deploys  
The Beer-Lambert’s Law via reflectance
  - + 3D digitizing by a nanoscanner
  - + 3D lattice creation (the BLR lattice) by “Inverse distance to power equations” algorithm (the reconstructive imaging)
- Combination of the three components produce  $< 1 \text{nm}$  resolution images

## Reconstructive imaging vs. camera



- As outlined in the above diagram, reconstructive imaging technique replaces the lens and the CCD by a nanoscanner and computer algorithm.
- Offers a huge zoom; from  $< 1 \text{nm}$  to centimeters.



© 2015—2018 Applied Research & Photonics

**Both reflection mode and transmission mode**



**Live demo at Lehigh University**

- Above: Terahertz nanoscanning spectrometer and 3D imager (TNS3DI)
- Right: Practical demo to a group

Applied Research & Photonics -- Proprietary -- 05/31/2016 (C) 2018 Anis Rahman  15

## Reconstructive Image generation

### Gridding with Inverse Distance to Power Equations

$$\hat{C}_j = \frac{\sum_{i=1}^n \frac{C_i}{h_{ij}^\beta}}{\sum_{i=1}^n \frac{1}{h_{ij}^\beta}} \quad (1)$$

where,  $h_{ij} = \sqrt{d_{ij}^2 + \delta^2}$ ,

$h_{ij}$  the effective distance between grid node  $j$  and the neighboring point  $i$ ;

$\hat{C}_j$  are the interpolated values for lattice node  $j$ ;

$C_i$  are the neighboring points;

$d_{ij}$  is the distance between grid node  $j$  and the neighboring point  $i$ ;

$\beta$  is the Power or weighting parameter; and

$\delta$  is the Smoothing parameter.

**Only Interpolation; NO Extrapolation**

1. Davis, John C. (1986) *Statistics and Data Analysis in Geology*. John Wiley and Sons, New York, NY.
2. Franke, R. (1982) *Scattered Data Interpolation: Test of Some Methods*, Mathematics of Computations, v. 33, n. 157, p. 181-200.

Applied Research & Photonics -- Proprietary -- 05/31/2017 (C) 2018 Anis Rahman  16

## General procedure

### 1. Imaging

- a) Determine resolution requirement (lowest is 25 nm)
- b) Scan the sample: XY, XYZ, XY $\theta$ , XYZ $\theta$ , etc.
- c) Generate image by the inverse gridding (supplied software)
- d) Analyze image for surface, volume (3D), layer-by-layer, contour, iso-surface, etc.

## Data structure

### Requirements

For every  $Z_1: Y_1 \dots Y_n;$   
 ...  
 for every  $Y_n: X_1 \dots X_n$   
 For every  $Z_2: Y_1 \dots Y_n;$   
 ...  
 for every  $Y_n: X_1 \dots X_n$   
 ...  
 ...  
 ...  
 For every  $Z_n: Y_1 \dots Y_n;$   
 ...  
 for every  $Y_n: X_1 \dots X_n$

Data are defined by:  $3 \times m$  matrix

Data file looks like:

x1	y1	z1	v1
...	.	z1	⋮
xn	y1	z1	⋮
x1	y2	z1	⋮
...	.	z1	⋮
xn	y2	z1	⋮
...	...	...	...
x1	yn	z1	⋮
...	.	z1	⋮
xn	yn	z1	⋮
...	...	...	...
x1	y1	zn	⋮
...	.	.	⋮
xn	yn	zn	v $\infty$

## Calculation illustration

Assume a function,

$$f(x, y, z) = c * \sin(x)$$

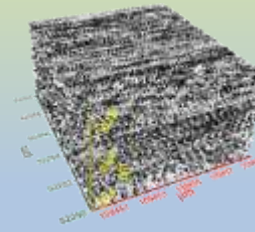
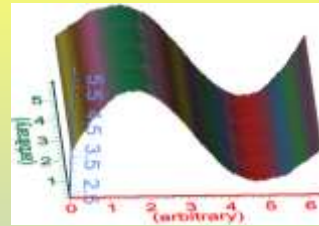
Let's calculate this function over the 3D space:

$X \rightarrow 0 \dots 2\pi$ ;  $y \rightarrow 0 \dots 6$ ;  $z \rightarrow 0 \dots 6$

Now one can construct the data space. Then use a gridding method to reconstruct (map) the function over the given 3D space. The plot looks like as shown.

Closer the grid points, smoother will be the surface.

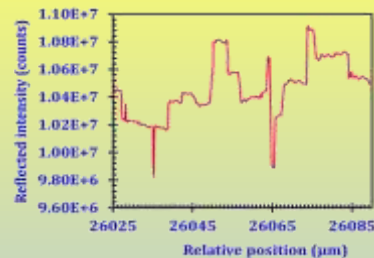
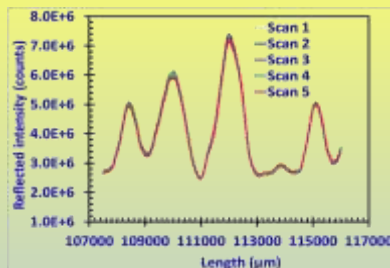
One can plot experimental data by the same procedure.



Raw data corresponding to a 3D scan does not yield meaningful information  
→ Not simple tomography or topography

(C) 2018 Anis Rahman

## Intensity based image contrast



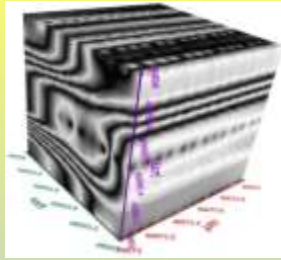
$$\Delta I \propto \Delta(X, Y, Z)$$

- Reproducibility of the traces.
- Reflected Intensity ( $I$ ) is  $\propto$  to material property. This forms the basis for nanometer resolution imaging.

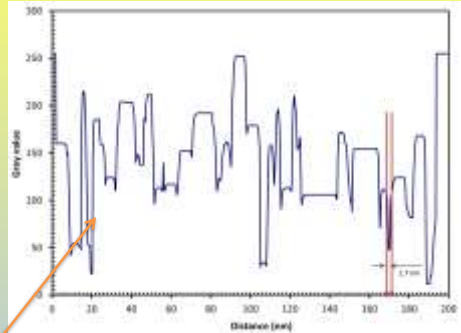
Beer-Lambert's law is rewritten as:  $\Delta I = \alpha l \epsilon(x, y, z)$

$\alpha$ : the molar absorptivity  
 $l$ : the path length, and  
 $\epsilon$ : the dielectric constant

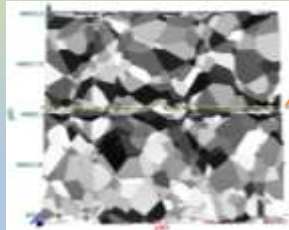
## Example: Cr<sup>3</sup> nanoparticles on glass slide



3D image of 1 cubic micron Cr<sup>3</sup> film

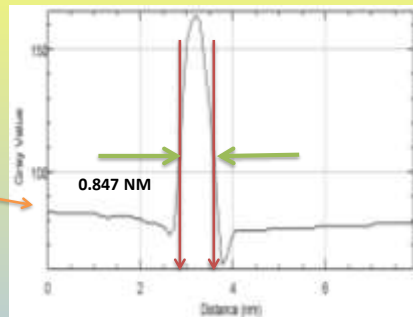
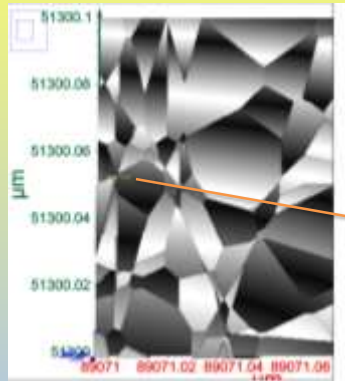


Analysis along the yellow line shows the smallest particle size ~ 1.7 nm.



200 nm x 200 nm close-up of a surface

## High Resolution Analysis

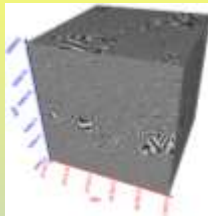
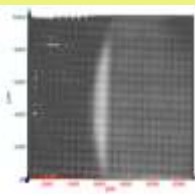


Cr<sup>3</sup> nanoparticles on glass slide. Smallest particle detected is ~8.5Å (<1 nm).

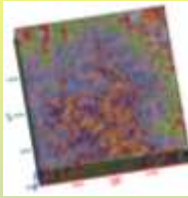
## Practical examples and comparison with other techniques

1. A plane mirror
2. Patterned wafer
3. Nanometer metal lines on 3D chip
4. Alumina nano-structure and nano-voids
5. Nano-suspension (slurry)
6. Quantum dots
7. Epitaxial semiconductor layers
  - stacking fault, dislocation
8. Stress induced lattice defect in GaN
9. Graphene
10. Carbon nanotube
11. Soft tissue

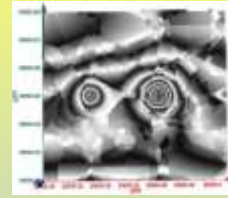
## Nano image examples

Alumina (50x50 nm<sup>2</sup>)

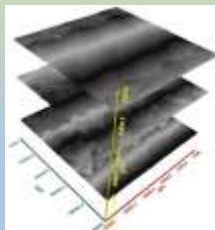
Patterned wafer



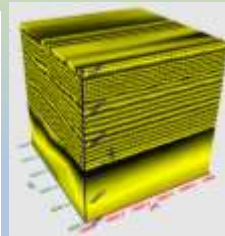
A single die



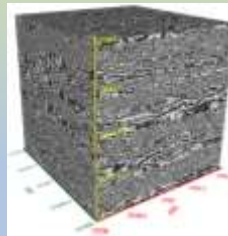
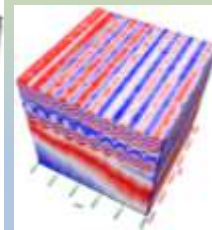
Two adjacent Gold nanoparticles



Layer by layer analysis

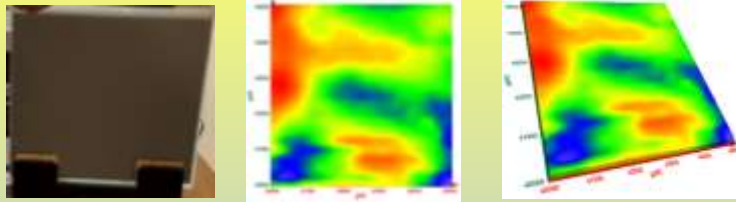


Epitaxial Semiconductor lattice structure

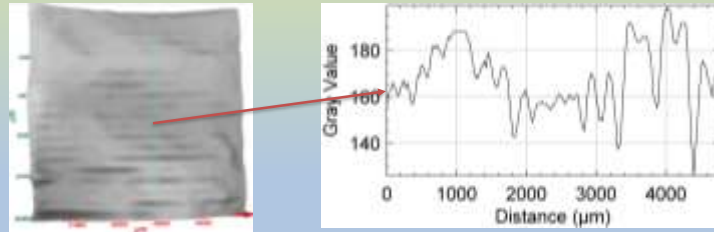
GaN lattice damage (2x2x2 μm<sup>2</sup>)

Carbon nanotubes (60°)

## A plane mirror



From left: A mirror mounted for imaging, surface roughness, 3D surface image

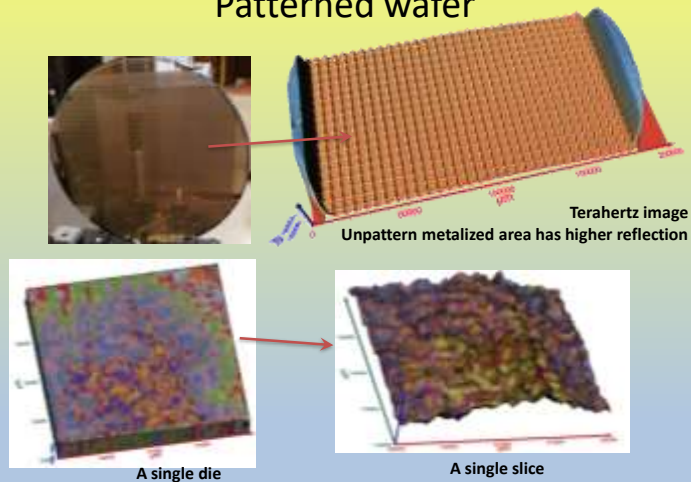


From left: Metallization seen through glass, surface roughness of the metal layer

(C) 2018 Anis Rahman

25

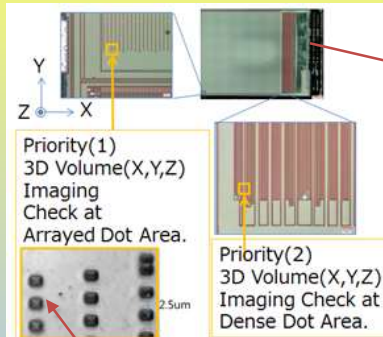
## Patterned wafer



(C) 2018 Anis Rahman

26

# Metal lines on a 3D chip



SEM image of dot pattern

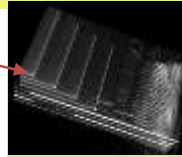


Photo of the actual sample

- Stack of 4 chips (about 100 μm each) on other patterned substrate
- Many high aspect arrayed dots (hole pattern) on each chip
- About 50 layers total

(C) 2018 Anis Rahman

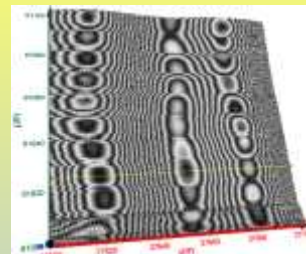


27

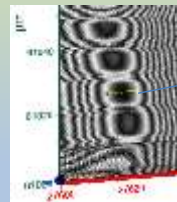
# Terahertz image: Task 1 - the dot pattern



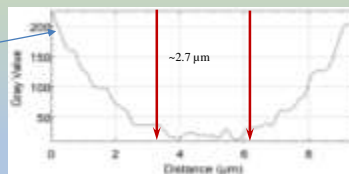
3D image reveals the dot pattern



Surface image of the dot pattern



Quantifying a single dot.



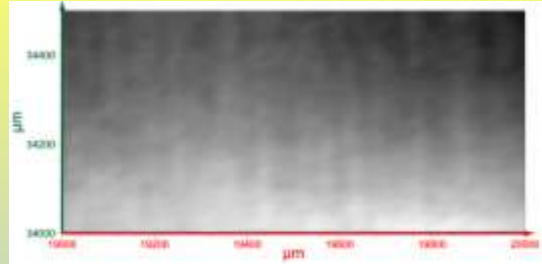
A representative dot is ~2.7 μm

(C) 2018 Anis Rahman

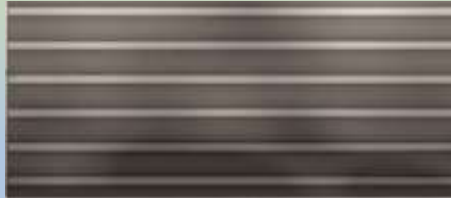


28

## Terahertz image: lines pattern



Large area view, lines are not visible



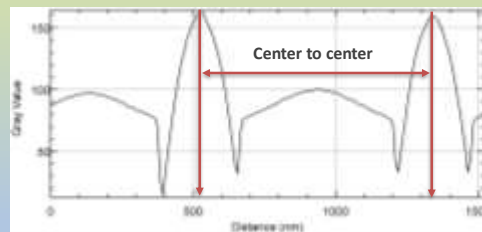
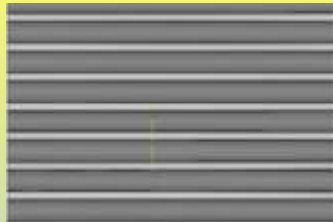
Zooming over 200  $\mu\text{m}$  x 90  $\mu\text{m}$  area reveals the nano-lines

(C) 2018 Anis Rahman

APPLIED RESEARCH &  
PHOTONICS

29

## Terahertz image: Pitch definition



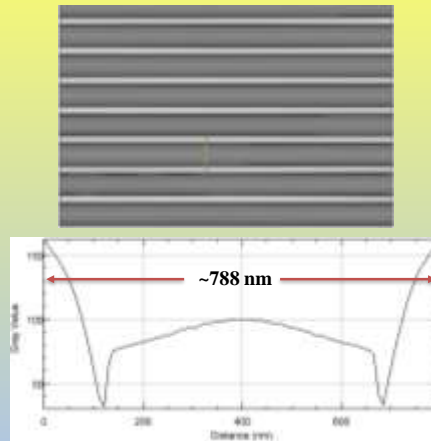
Pitch = Center-to-center distance between two adjacent lines

(C) 2018 Anis Rahman

APPLIED RESEARCH &  
PHOTONICS

30

## Terahertz image: Measured Pitch



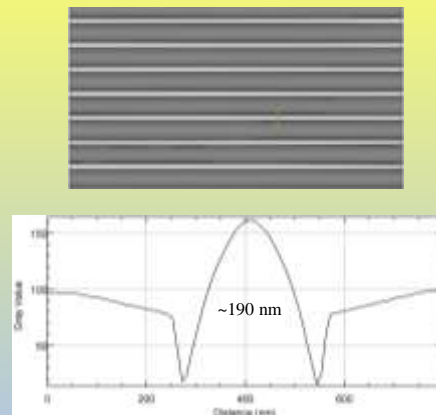
Measured center-to-center distance between two adjacent lines = 788 nm

(C) 2018 Anis Rahman

APPLIED RESEARCH &  
PHOTONICS

31

## Terahertz image: Linewidth measured



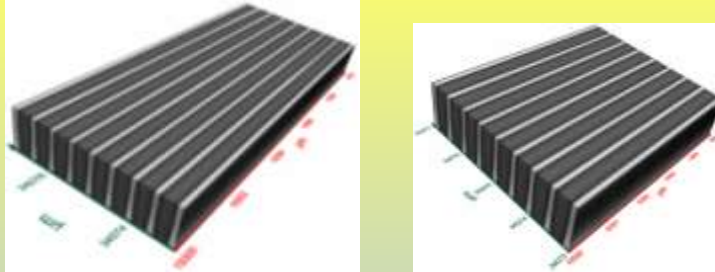
Measured width of a single line = 190 nm

(C) 2018 Anis Rahman

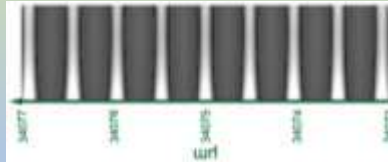
APPLIED RESEARCH &  
PHOTONICS

32

## Terahertz image: 3D view of lines



3D views of two different angles (SEM/TEM cannot see this)



YZ-plane view from above (slightly enlarged).  
Each line has visible aspect ratio (SEM/TEM cannot see this)

(C) 2018 Anis Rahman

APPLIED RESEARCH &  
PHOTONICS

33

## Comparison with SEM data

Table 1. Comparison between SEM and Terahertz results

Observable	SEM	Terahertz	%disagreement*
Line pitch	~760 nm	~780 nm	2.63
Line width	~160 nm	~190 nm	18.75
Thickness	3.5 $\mu\text{m}$	~3.5 $\mu\text{m}$	~0
Dot size	~133 nm	~131.3 nm	-1.28
Dot pitch (vertical)	~48 nm	~53.1 nm	10.6

\*% disagreement = (new\_value - original\_value)/ABS(original\_value)

- The differences are due to the aspect ratio of the lines (SEM cannot see this)

(C) 2018 Anis Rahman

APPLIED RESEARCH &  
PHOTONICS

34

## Nanoparticles in suspension

### Procedure:

- A small path-length cuvette
- Mounted on the nanoscanner.
- Total volume of nano-suspension is ~1 mL.



The thickness of nano-suspension is shown by red arrows.

ORGANO SILICASOL™	Particle Size (nm)	SiO <sub>2</sub> (wt%)	H <sub>2</sub> O%	Viscosity (mPa.s.)	Specific Gravity	pH	Solvent
IPA-ST	10-15	30-31	< 1.0	< 15	0.96-1.02	2-4	IPA
CAS#	7631-86-9. Ref: <a href="https://www.nissanchem-usa.com/products/organosilicasol/">https://www.nissanchem-usa.com/products/organosilicasol/</a>						

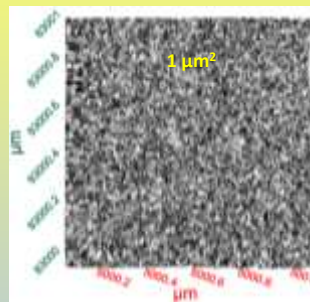
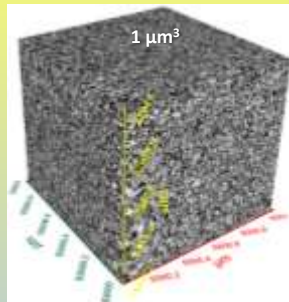
Nano-suspension properties as supplied by the Vendor.

(C) 2018 Anis Rahman

APPLIED RESEARCH &  
PHOTONICS

35

## Terahertz image of Blank cuvette



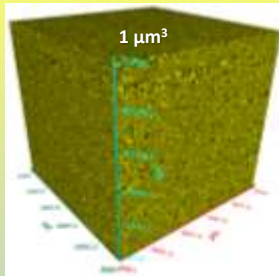
Blank cuvette exhibits amorphous structure

(C) 2018 Anis Rahman

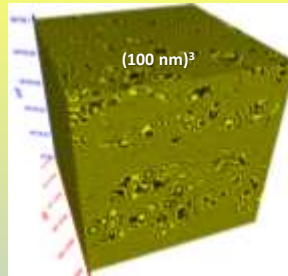
APPLIED RESEARCH &  
PHOTONICS

36

## Terahertz image of Nano-suspension



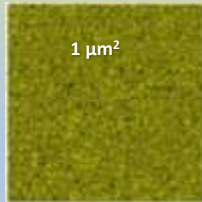
More or less homogeneous suspension



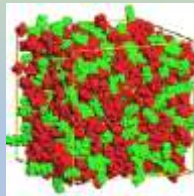
A close up reveals formation of nano-agglomeration

Partial agglomeration visible

Nano-clusters, ~18 nm



More or less homogeneous suspension



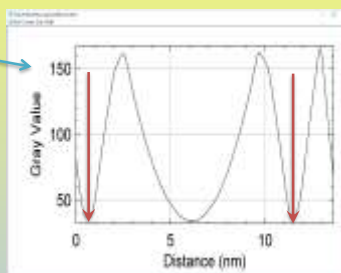
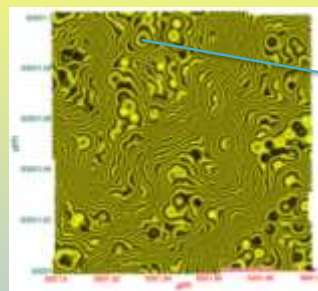
Simulation of nano-agglomerates (green) in suspension

(C) 2018 Anis Rahman

APPLIED RESEARCH &  
PHOTONICS

37

## Terahertz image zoomed for single particle size determination



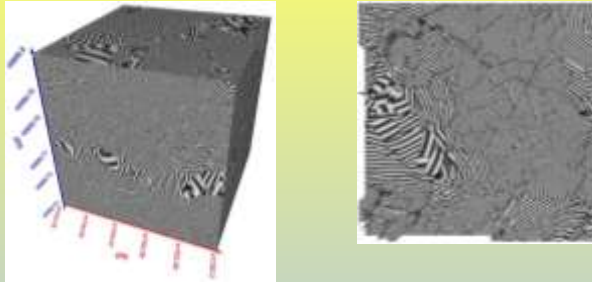
Single particle size ~10.75 nm

(C) 2018 Anis Rahman

APPLIED RESEARCH &  
PHOTONICS

38

## Terahertz image of nano-grains and nano-voids in Alumina



Terahertz image of alumina showing nano-grains. 3D (left), and 2D (right) images

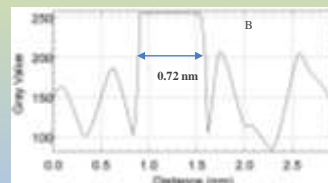
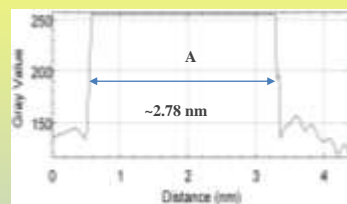
- High purity alumina bioceramics serve as an alternative to surgical metal alloys
- Used for total hip prosthesis and tooth implants
- High hardness, low friction coefficient and corrosion resistant
- Alumina offers a very low wear rate at the articulating surfaces in orthopedic applications
- Better understanding of its nanostructure is important

(C) 2018 Anis Rahman

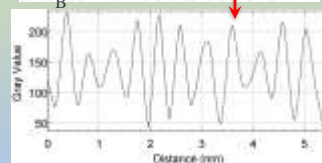
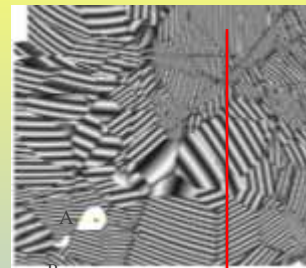
APPLIED RESEARCH &  
PHOTONICS

39

## Nano nano-voids in Alumina quantified



Nanovoids: A ~2.78 nm, B ~0.72 nm



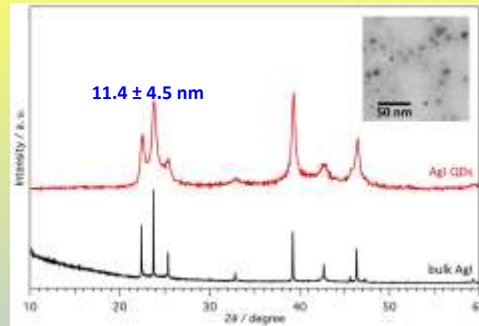
Detailed structure of a nano-grain

(C) 2018 Anis Rahman

APPLIED RESEARCH &  
PHOTONICS

40

## Terahertz imaging of quantum dots

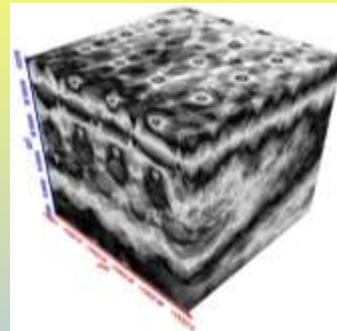


PXRD and TEM analysis shows the AgI quantum dots are  $(11 \pm 4.5)$  nm.

Ref: Rahman, A.; Rahman, A. K.; Yamamoto, T.; Kitagawa, H., "Terahertz sub-nanometer sub-surface imaging of 2D materials." J. Biosens. Bioelectron., 2016, 7:3

## AgI quantum dots terahertz image

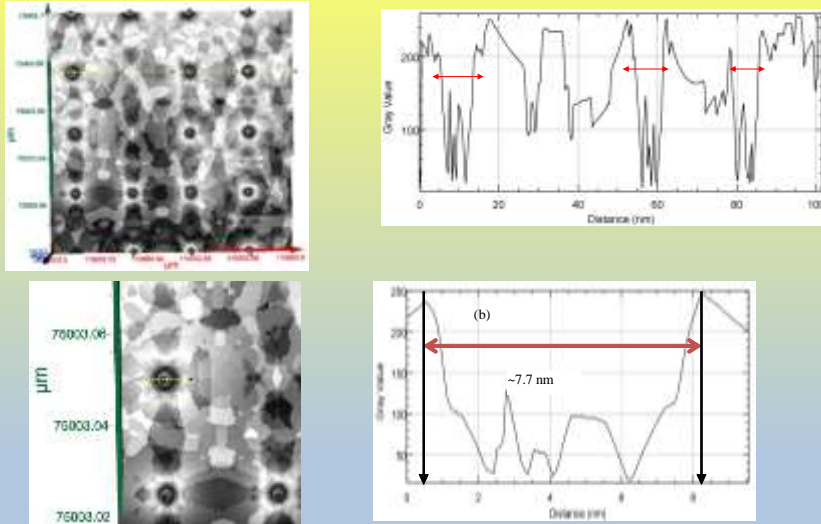
- AgI quantum dots were received from Kyoto University
- As received samples were dispersed in MeOH, spun on Si wafer
- Scanned and imaged by terahertz nanoscanner /spectrometer (TNS3DI) [1]



100 nm<sup>3</sup> volume (close up) extracted from the 5 μm<sup>3</sup> scanned volume.

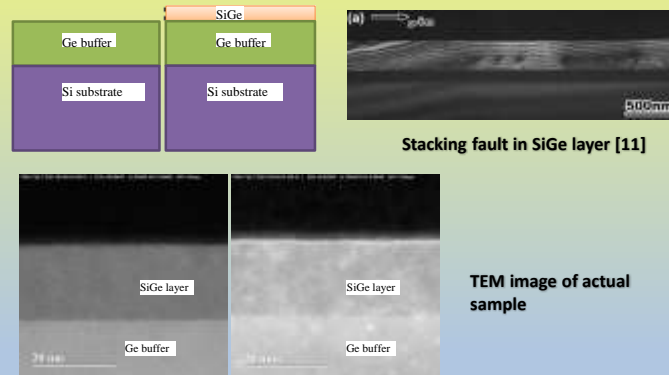
[1] Rahman, A.; Rahman, A. K.; Yamamoto, T.; Kitagawa, H., "Terahertz sub-nanometer sub-surface imaging of 2D materials." J. Biosens. Bioelectron., 2016, 7:3

## QD size analysis from terahertz image

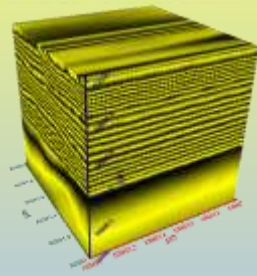


Ref: A. Rahman, H. Kitagawa et al., J Biosens Bioelectron 2016, 7:3  
 DOI: 10.4172/2155-6210.1000221

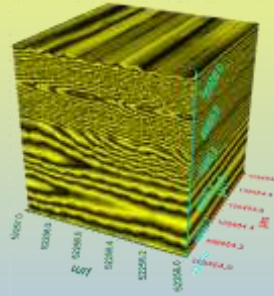
## Epitaxial Semiconductor



### 3D image of Ge & SiGe



1 μm³ volume of D02

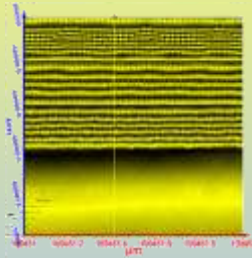


1 μm³ volume of D10

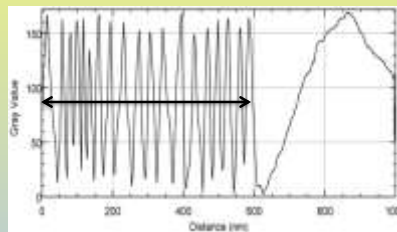
Ref: Rahman and Rahman, J Biosens Bioelectron 2016, 7:4  
DOI: 10.4172/2155-6210.1000229

Applied Research & Photonics -- Proprietary -- 05/31/2017

### Ge Layer thickness



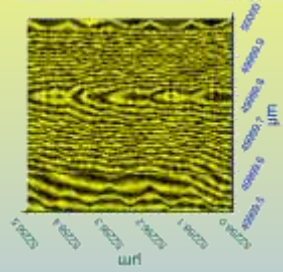
D02: one square micron face (XZ surface) extracted from volume



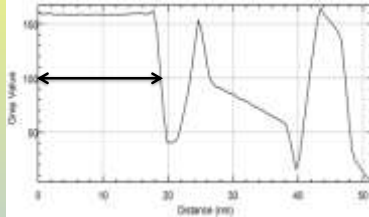
Graphical analysis along the vertical line of sample D10. Measured thickness of the Ge layer is ~ 590 nm (see arrow).

Applied Research & Photonics -- Proprietary -- 05/31/2017

## SiGe layer thickness

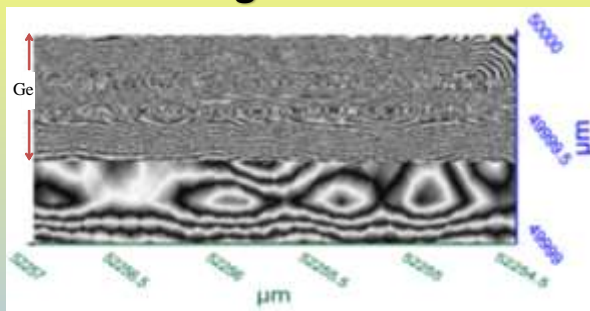


Sample D10: 500 nm square face (YZ surface) extracted from volume



Graphical analysis of sample D02 from the image. Measured thickness of the SiGe layer (top) is ~ 18 nm.

## Stacking fault in Ge

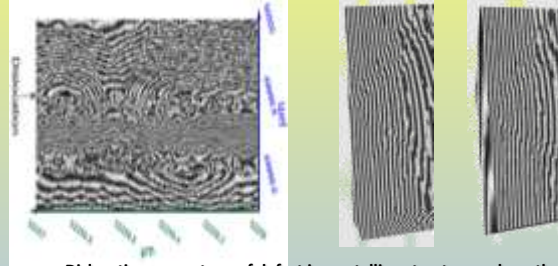


some non-uniformity is visible in the top layer thickness.

A stacking fault is a type of defect which characterizes the disordering of crystallographic planes.

Ref: A. Rahman, ASMC 2017, 978-1-5090-5448-0/17/\$31.00 ©2017 IEEE

## Dislocation

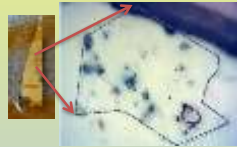


- Dislocations are a type of defect in crystalline structures where the atoms are out of position in the lattice.
- Dislocations are generated and move as a result of an applied stress.

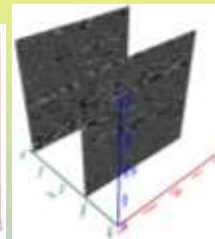
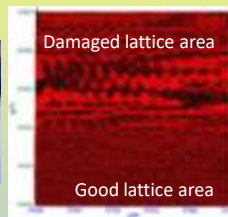
Applied Research & Photonics -- Proprietary -- 05/31/2017

(C) 2018 Anis Rahman

## GaN and Layer by layer



GaN grown on Silicon  
damaged by high electric field stress



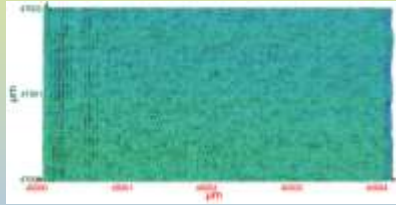
Samples courtesy of Dr. A. Haque of PSU

Applied Research & Photonics -- Proprietary -- 05/31/2017

(C) 2018 Anis Rahman

## Terahertz image of graphene exfoliates

- Dilute solution of graphene
- Spun on Si wafer
- 3D scanning and imaging
- Exfoliate layers may be quantified



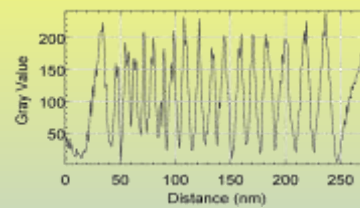
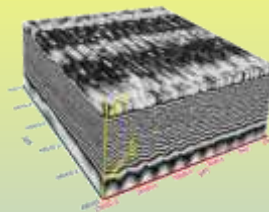
2  $\mu\text{m}$  x 4  $\mu\text{m}$  surface image of graphene on wafer (sample: 7-12-N graphene solution in NMP).

(C) 2018 Anis Rahman

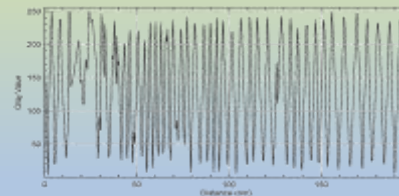
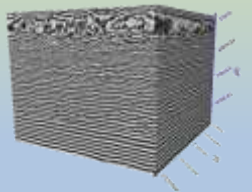
51

## Graphene exfoliates comparison

**Sample: 7-12-N**  
Smallest  
exfoliate  
thickness ~1  
nm



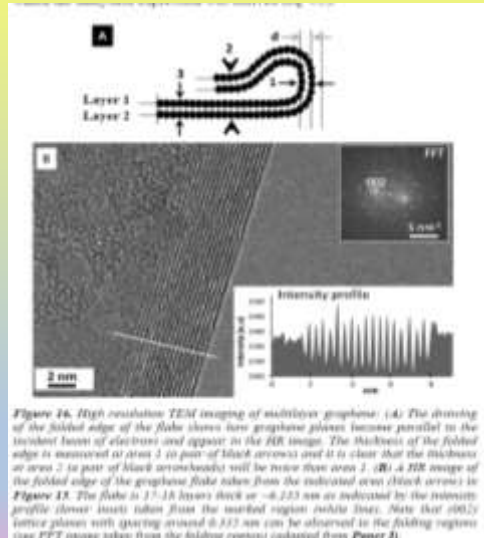
**Sample: G95-N**  
Smallest  
exfoliate  
thickness <1  
nm



## Graphene Exfoliates reference

Ref. "TEM of Graphene & Hydrated Biomaterial Nanostructures," Sultan Akhtar, 2012, Dissertation, Uppsala Univ., ISBN: 978-91-554-8333-3; ISSN: 1651-6214

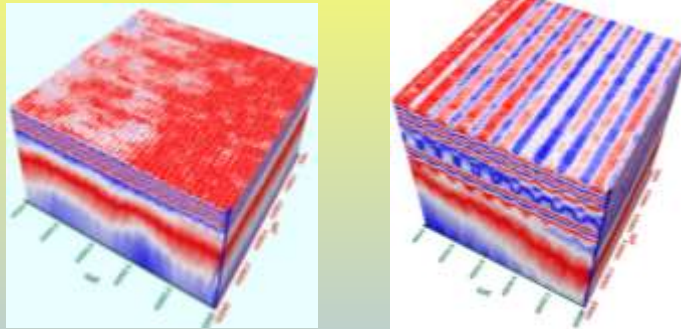
17–18 layers



(C) 2018 Anis Rahman

APPLIED RESEARCH & PHOTONICS

## Carbon nanotubes

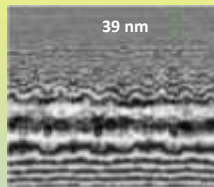


3D images of carbon nanotubes spun on Si wafer. Left: Unaligned; right: Aligned @ 60°

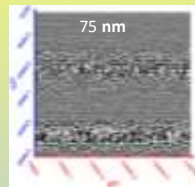
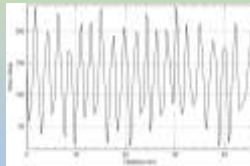
Samples courtesy of Prof Junichiro Kono, Rice Univ.

## Carbon nanotubes (contd.)

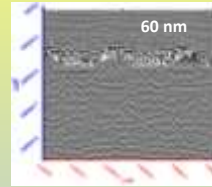
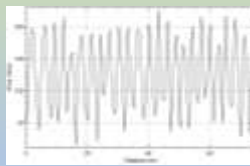
Variation in layer thickness as a function of alignment of CNT film spun and aligned on Si wafer



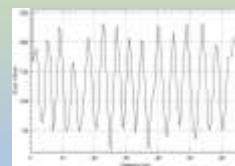
Unaligned



60° aligned



167° aligned



(C) 2018 Anis Rahman

APPLIED RESEARCH &  
PHOTONICS

55

## Conclusions

APPLIED RESEARCH &  
PHOTONICS

- Abbe Diffraction limit has been overcome by terahertz multispectral reconstructive imaging as implemented
- Achieved sub-nanometer image resolution with terahertz radiation in the X, Y, and Z directions
- Combination of a smart nanoscanning spectrometer and algorithm replaces a CCD for sub-nanometer resolution
  - Non-destructive, Non-contact, sub-surface, layer-by-layer
  - Inspect 0D, 1D, 2D and 3D materials
  - Lattice defects, stacking faults
  - Defects, cracks, non-uniformity, inclusion, phases, etc.
- Several nanosystem have been investigated for quantitative measurement and visual inspection.

Applied Research & Photonics -- Proprietary -- 05/31/2017

(C) 2018 Anis Rahman

APPLIED RESEARCH &  
PHOTONICS

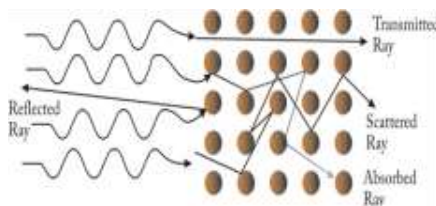
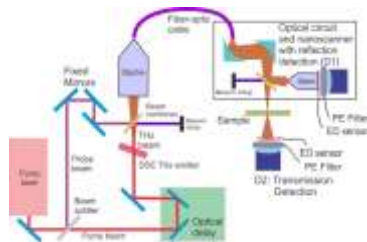
56

## Conclusions – terahertz imaging

- **Abbe Diffraction limit has been overcome by terahertz multispectral reconstructive imaging as implemented**
- **Achieved sub-nanometer image resolution with terahertz radiation in the X, Y, and Z directions**
- **Combination of a smart nanoscanning spectrometer and algorithm replaces a CCD for sub-nanometer resolution**
  - Non-destructive, Non-contact, sub-surface, layer-by-layer
  - Inspect 0D, 1D, 2D and 3D materials
  - Lattice defects, stacking faults
  - Defects, cracks, non-uniformity, inclusion, phases, etc.
  - Layer thicknesses, delamination
- **Several nanosystems have been investigated for quantitative measurement and visual inspection.**

## Terahertz Spectroscopy

# Principle of THz Spectroscopy



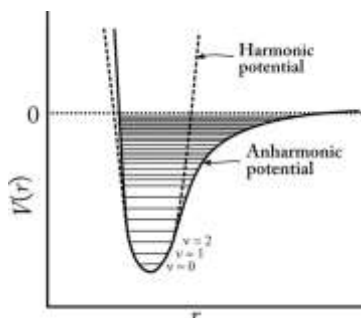
- THz radiation stimulates many resonances (in general molecular “events”), resulting in the THz photons being affected by characteristic amounts determined by a specific interaction or event.
- The change in energy yields information about the molecular nature of the interaction.
- Infrared and Raman spectroscopy yields similar information but not capable of detecting many resonant states as can be detected with THz.
- Spontaneous Raman scattering is typically very weak, as a result the main difficulty of Raman spectroscopy is in resolving the weak inelastically scattered light from the intense Rayleigh scattered laser light.

Applied Research & Photonics -- Proprietary -- 03/03/2017

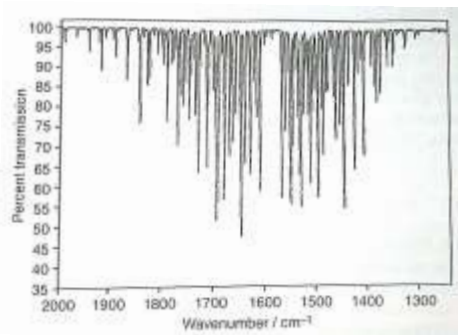
APPLIED RESEARCH & PHOTONICS

59

## Higher Sensitivity



Potential energy of a diatomic molecule as a function of displacement during a vibration



Vibration-rotation spectrum of H-O-H bending mode of water vapor

**Higher sensitivity is required to sense more “states”**

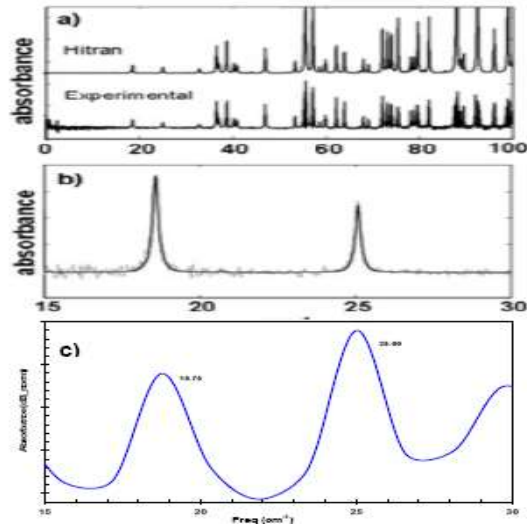
Ref: Griffiths & de Haseth, Fourier Transform Infrared Spectroscopy, Wiley 2007

Applied Research & Photonics -- Proprietary -- 03/03/2017

APPLIED RESEARCH & PHOTONICS

## Do the validation

Water vapor absorption spectrum obtained using the THz spectrometer compared to that calculated using the HITRAN database by the NIST. An expanded portion in the panel (b) containing pressure broadened water lines from NIST (c): Expanded view of vapor absorption lines obtained from ARP's TeraSpectra (see Fig. 5). Low frequency peaks match well with those reported by the NIST [1].



1. <http://arphotronics.net/WaterVaporComparison1.pdf>

Applied Research & Photonics -- Proprietary -- 03/03/2017

APPLIED RESEARCH & PHOTONICS

## Experimental Setup



Sample mount on the integrated terahertz nanospecting spectrometer. Sample may be of any shape. Fiber coupled beam delivery allows vertical incidence in any direction.

Applied Research & Photonics -- Proprietary -- 03/03/2017

APPLIED RESEARCH & PHOTONICS

## Sample considerations

---

- **Samples may be solid, liquid or gaseous**
- **Solids may be mounted directly**
- **Many solids are dissolved and formed in to film on a suitable substrate**
- **Different cuvettes may be used for liquid samples**
- **Gaseous may be measured, either stationary or under flowing**
- **Both reflection and/or transmission measurements**

## Measurement mode

---

1. **Spectroscopy**
  - a) **Reflection, transmission, stand-off distance**
2. **Imaging**
  - a) **Reflection, transmission, transreflectance, one parameter, multi-parameter**
3. **Thickness profiling**
  - a) **Mostly reflection, may be transmission or transreflection.**

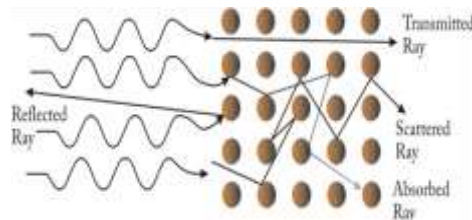
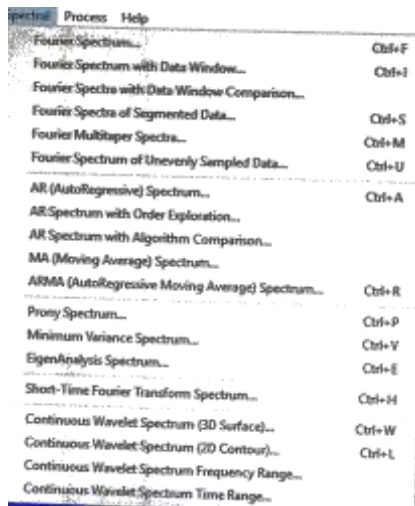
## General procedure

1. Spectroscopy
  - a) Mount sample
  - b) Acquire spectrum
  - c) Do Fourier transform
  - d) Analyze spectrum
2. Thickness profiling
  - a) Mount sample
  - b) Determine suite spot and scan resolution requirement
  - c) Perform 1D scanning
  - d) Analyze profile by Microsoft Excel
3. Interpret results (on your own?)

Applied Research & Photonics -- Proprietary -- 03/03/2017

APPLIED RESEARCH &  
PHOTONICS

## Spectra generation and analysis



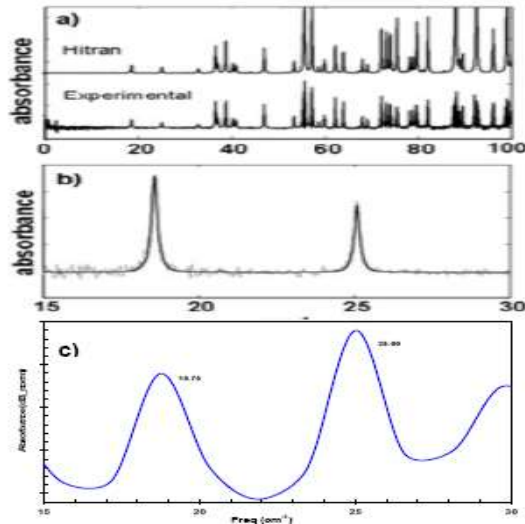
- Choose the right transform (skill, trial and error)
- Identify background peaks
- Interpret sample characteristics

Applied Research & Photonics -- Proprietary -- 03/03/2017

APPLIED RESEARCH &  
PHOTONICS

## Spectrometer Validation

Water vapor absorption spectrum obtained using the THz spectrometer compared to that calculated using the HITRAN database by the NIST. An expanded portion in the panel (b) containing pressure broadened water lines from NIST (c): Expanded view of vapor absorption lines obtained from ARP's TeraSpectra (see Fig. 5). Low frequency peaks match well with those reported by the NIST [1].

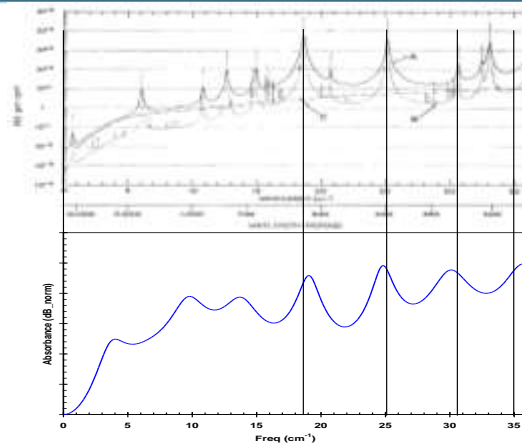


1. <http://arphotonics.net/WaterVaporComparison1.pdf>

Applied Research & Photonics -- Proprietary -- 03/03/2017

APPLIED RESEARCH &  
PHOTONICS

## Spectra analysis examples: water spectrum

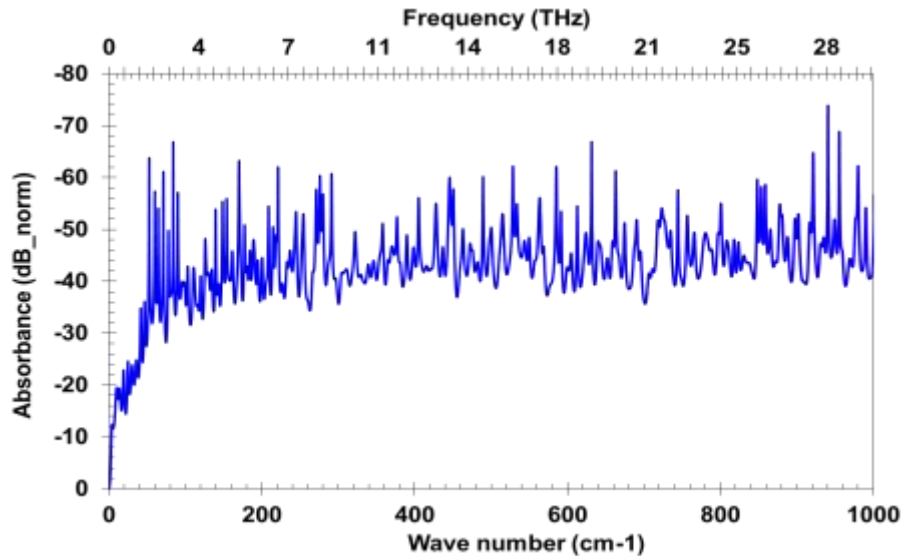


Ref. Darrell Burch, "Absorption of Infrared Radiant Energy by CO<sub>2</sub> and H<sub>2</sub>O. III. Absorption by H<sub>2</sub>O between 0.5 and 36 cm<sup>-1</sup> (278 u-2 cm)," Journal of the Optical Society of America, 58 (#10), 1383, 1968.

Applied Research & Photonics -- Proprietary -- 03/03/2017

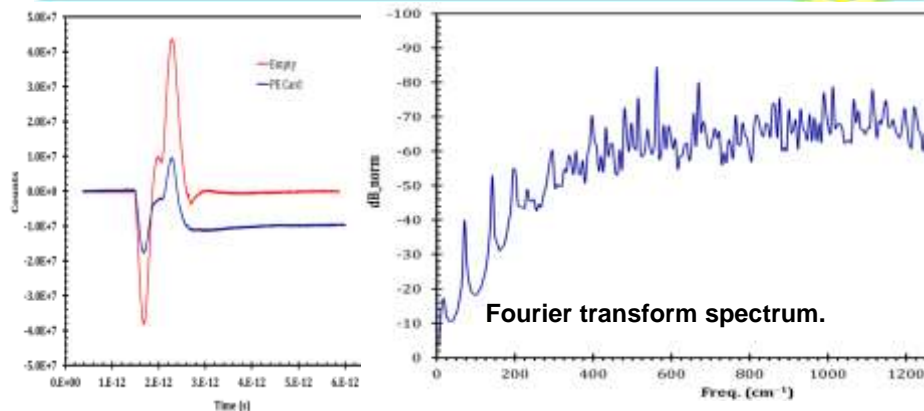
APPLIED RESEARCH &  
PHOTONICS Anis Rahman

## Water spectrum up to ~30 THz



Applied Research & Photonics -- Proprietary -- 03/03/2017  8 Anis Rahman

## PE time-domain spectrum

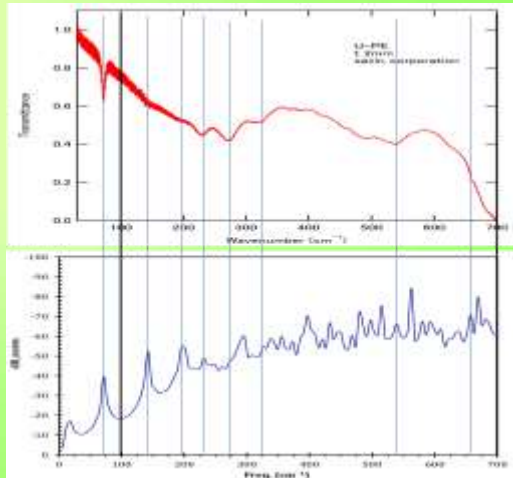


- Terahertz reproduced absorbance peaks known from other methods
- Many peaks not visible previously were discovered.

Applied Research & Photonics -- Proprietary -- 03/03/2017 

# Matching peaks

Ref.	Reported (1/cm)	TeraSpectra (1/cm)
14	70.8	71
15		142.1
		195.4
		230.9
		272.4
		325.7
16	723.3	722.5
	749.5	746.2
	1466.02	1457, 1469
	1492.23	1486.4, 1510

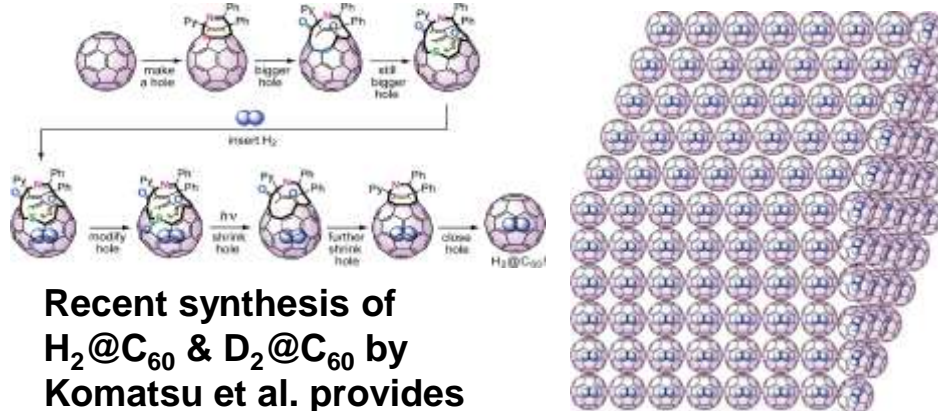


14. Polyethylene spectrophotometric grade, SIGMA-ALDRICH. <http://thzdb.org/image.php?image=000000773>  
 15. THZ database: <http://thzdb.org/index.php?name=White&word=polyethylene>  
 16. FreeSnell: Polyethylene <http://people.csail.mit.edu/jaffer/FreeSnell/polyethylene.html>

Applied Research & Photonics -- Proprietary -- 03/03/2017

APPLIED RESEARCH & PHOTONICS

## $C_{60}$ , $H_2@C_{60}$ & $D_2@C_{60}$

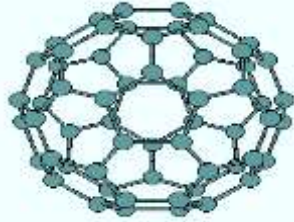


Recent synthesis of  $H_2@C_{60}$  &  $D_2@C_{60}$  by Komatsu et al. provides opportunity to investigate the properties of the endohedral Fullerenes

Applied Research & Photonics -- Proprietary -- 03/03/2017

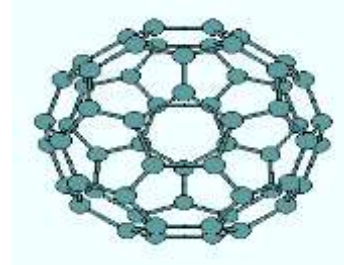
APPLIED RESEARCH & PHOTONICS

# Vibrational Modes of C<sub>60</sub>

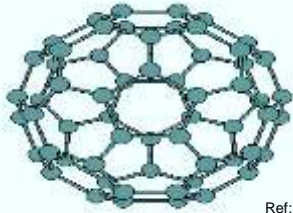


MODE	DEGENERACY	FREQ. (cm <sup>-1</sup> )
Hg(1)	5	272

Gh(1) 3 343



Gh(1) 4 353



Ref: [http://www.public.asu.edu/~cosmen/C60\\_vibrations/mode\\_assignments.htm](http://www.public.asu.edu/~cosmen/C60_vibrations/mode_assignments.htm)

Applied Research & Photonics -- Proprietary -- 03/03/2017

APPLIED RESEARCH & PHOTONICS

MODE	DEGENERACY	FREQ. (cm <sup>-1</sup> )
Hg(1)	5	272
T <sub>1g</sub> (1)	3	343
Gh(1)	4	353
Hu(1)	5	403
Hg(2)	5	433
Gh(1)	4	485
Au(1)	1	496
T <sub>1g</sub> (1)	3	526
Hu(2)	5	534
T <sub>1g</sub> (1)	3	553
Gh(2)	4	567
T <sub>1g</sub> (1)	3	568
T <sub>1g</sub> (2)	3	575
Hu(2)	5	668
Hg(3)	5	709
Gh(3)	4	736
Hu(4)	5	743
T <sub>1g</sub> (2)	3	753
T <sub>1g</sub> (2)	3	756
Gh(2)	4	764
Hg(4)	5	772
Gh(3)	4	776
T <sub>1g</sub> (3)	3	798

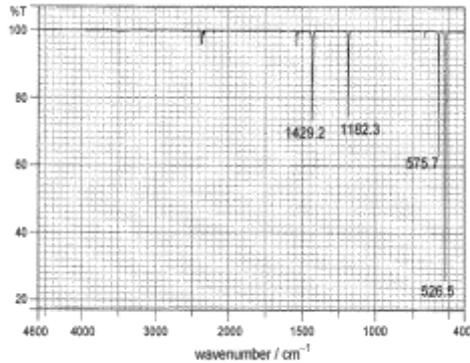
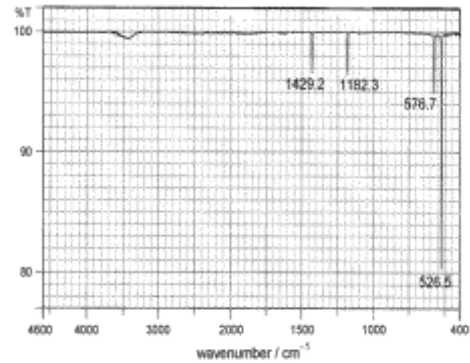
MODE	DEGENERACY	FREQ. (cm <sup>-1</sup> )
T <sub>1g</sub> (2)	3	831
Gh(4)	4	961
T <sub>1g</sub> (3)	3	973
Au	1	984
Gh(4)	4	1079
Hu(3)	5	1099
T <sub>1g</sub> (3)	3	1182
T <sub>1g</sub> (4)	3	1205
Hu(5)	5	1223
Hu(6)	5	1282
T <sub>1g</sub> (4)	3	1289
Gh(5)	4	1309
Gh(5)	4	1310
Hu(6)	5	1344
T <sub>1g</sub> (4)	3	1346
Gh(5)	4	1422
Hu(7)	5	1425
T <sub>1g</sub> (4)	3	1429
Au(2)	1	1470
Gh(5)	4	1482
T <sub>1g</sub> (5)	3	1525
Hu(7)	5	1567
Hu(8)	5	1575

Ref: [http://www.public.asu.edu/~cosmen/C60\\_vibrations/mode\\_assignments.htm](http://www.public.asu.edu/~cosmen/C60_vibrations/mode_assignments.htm)

Applied Research & Photonics -- Proprietary -- 03/03/2017

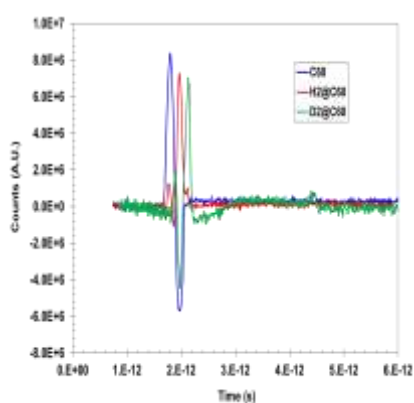
APPLIED RESEARCH & PHOTONICS

## IR spectra of $C_{60}$ & $H_2@C_{60}$

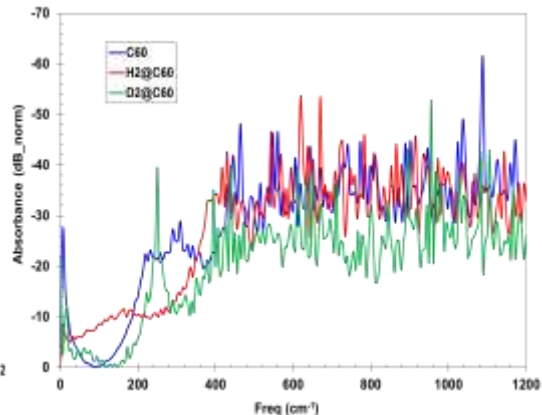
Figure S2 infrared spectrum (KBr) of  $C_{60}$ .Figure S1 infrared spectrum (KBr) of  $H_2@C_{60}$ .

Ref: Komatsu, K; Murata, M; Murata, Y (2005). "Encapsulation of molecular hydrogen in fullerene  $C_{60}$  by organic synthesis". *Science* 307 (5707): 238–40.

## Analysis of 3 Fullerenes



Time-domain signal of three Fullerenes.



Fourier transform absorption spectra of three Fullerenes.

## Comparison with theory

Comparison of IR and THz spectra of C <sub>60</sub> . All units are in cm <sup>-1</sup>	
C <sub>60</sub> : THz [present work]	C <sub>60</sub> : Ref. Menendez & Page, ASU
6.44, 219, 232, 258, 271, 290	272
309,328, 341, 361, 393	343, 353
406,432, 444, 464, 490	403,433, 485, 496
515,535, 543, 560, 593	526, 534, 553, 567, 568, 575
605,618, 644, 670	668
740, 772	709, 736, 743, 753, 756, 764, 772, 776, 796
857, 889	831
902, 947, 992	961, 973, 984
1024, 1037, 1088	1079, 1099
1127, 1159, 1172	1182
<b>Total: 38</b>	<b>30</b>

### Terahertz provides tool for details study of vibrational states

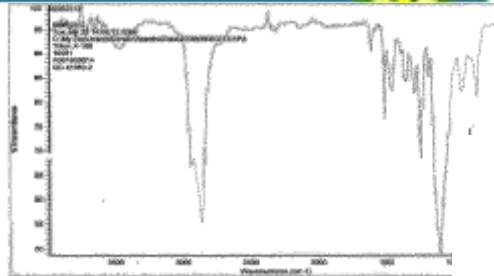
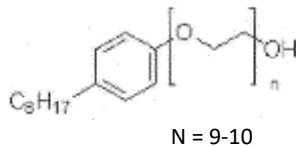
J. Menendez & J. B. Page, "Vibrational Spectroscopy of C<sub>60</sub>." [http://www.public.asu.edu/~cosmen/C60\\_vibrations/newc60revcorr.pdf](http://www.public.asu.edu/~cosmen/C60_vibrations/newc60revcorr.pdf)  
 "The vibrational modes of buckminsterfullerene C<sub>60</sub>" [http://www.public.asu.edu/~cosmen/C60\\_vibrations/mode\\_assignments.htm](http://www.public.asu.edu/~cosmen/C60_vibrations/mode_assignments.htm)

Applied Research & Photonics -- Proprietary -- 03/03/2017

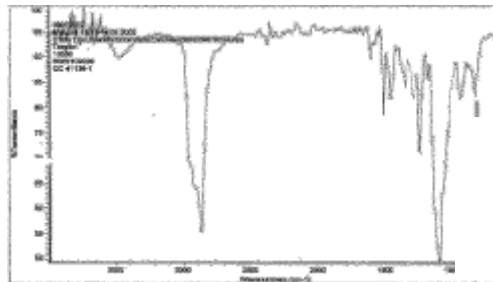
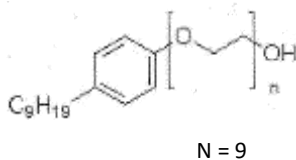
APPLIED RESEARCH &  
PHOTONICS

## Non-Ionic Detergents

- X-100



- NP-9



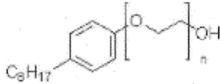
Applied Research & Photonics -- Proprietary -- 03/03/2017

APPLIED RESEARCH &  
PHOTONICS

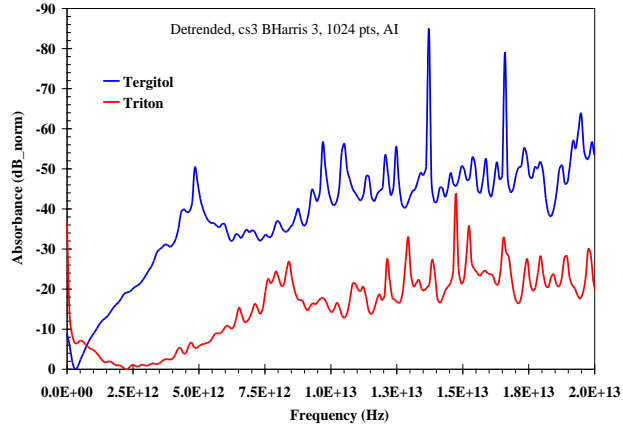
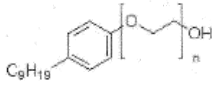
78

# Terahertz spectra reveal differences

- **X-100**

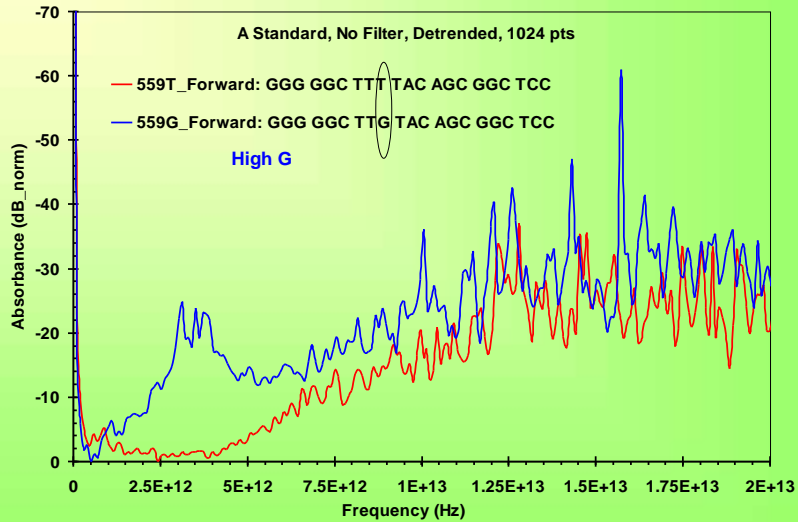


- **NP-9**

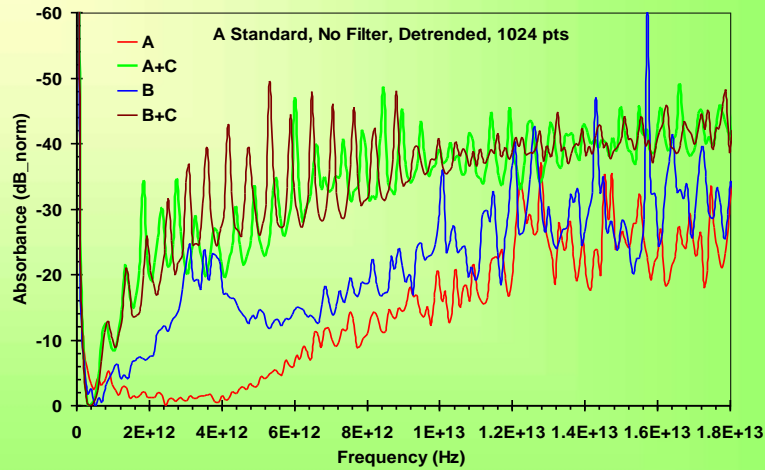


Liquid phase detergent in Plexiglas cuvette

## Spectra of Oligos with or without SNP (T>G)



## Single Strand vs. Double Strand Oligos



- A). 559T\_Forward: GGG GGC TTT TAC AGC GGC TCC  
 B). 559G\_Forward: GGG GGC TTG TAC AGC GGC TCC  
 C). 559T\_Reverse: GGA GCC GCT GTA AAA GCC CCC

Applied Research & Photonics -- Proprietary -- 03/03/2017

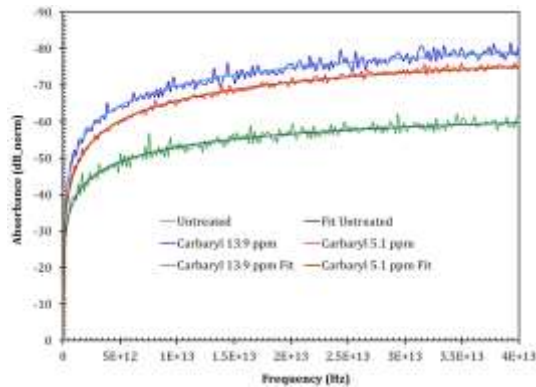
APPLIED RESEARCH & PHOTONICS

81

## Pesticide in fruits



Apple mounted in the spectrometer



Fourier transform absorbance (normalized) spectra of three samples along with their numerical fit.

$$y = a + b * \ln(x) + c * [\ln(x)]^2 + d * [\ln(x)]^3 + e * [\ln(x)]^4$$

Applied Research & Photonics -- Proprietary -- 03/03/2017

APPLIED RESEARCH & PHOTONICS

Anis Rahman82

## Pesticide in produces



Signature peak summary (THz)

Untreated Apple	Carbaryl 5.1 ppm	Carbaryl 13.9 ppm	
2.99	2.99	2.99	← Common for this apple
5.91	9.53	6.86	
12.52	13.96	13.13	← Carbaryl signature?
21.43	16.06	16.19	

Applied Research & Photonics -- Proprietary -- 03/03/2017

APPLIED RESEARCH & PHOTONICS

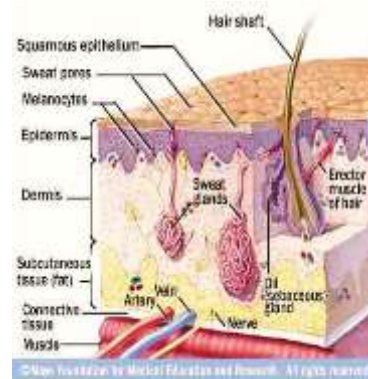
83

## Thickness profiling

(C) 2018 Anis Rahman

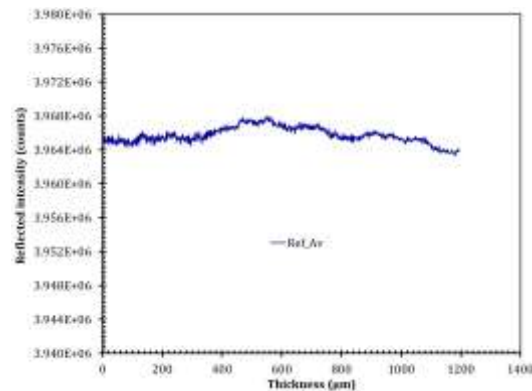
## Thickness profile: Layered structure of skin

- **Right: anatomical features of human skin cross section.**
- **A vertical scan (thickness profile) is expected to exhibit layering information.**
- **The layering pattern will be different at different spots on the skin because the thickness profile is not the same at every place.**
- **It is expected that a layered pattern of some kind will be present for the benign skin while the cancerous skin will exhibit diminished layered structure due to cell agglomeration and loss of regular cellular pattern.**



(C) 2018 Anis Rahman

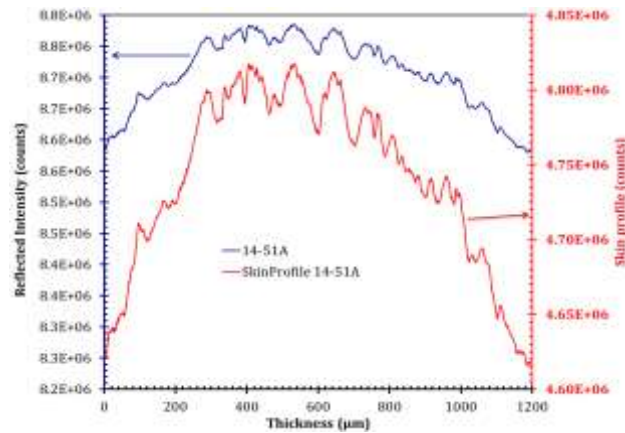
## Calibration of the sample holder



**Thickness profile of empty cell of high density polyethylene (HDPE) used as the reference. Several trials were taken that were averaged to obtain the Ref\_Av. Average error limit was calculated to be 2295 counts**

(C) 2018 Anis Rahman

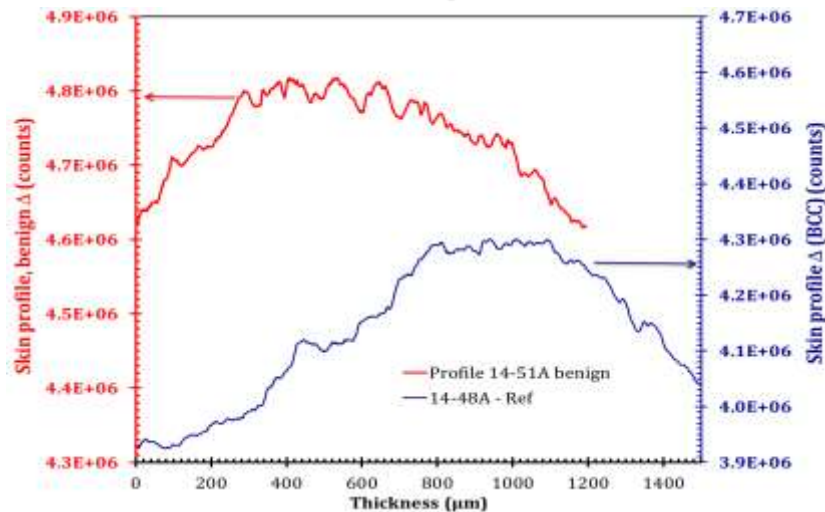
## Reflectance → layers of skin



Thickness profile from scan of a benign skin sample (14-51A, left Y-axis). The skin thickness profile (right Y-axis) is obtained by subtracting the reference.

(C) 2018 Anis Rahman

## Thickness profile



(C) 2018 Anis Rahman

## Terahertz scanning reflectometry

- Measurement of concentration gradient in a non-invasive (non-destructive) way is important in areas such as transdermal drug delivery.
- However, to our knowledge, there is no direct method to obtain two critical factors:
  - the concentration gradient of permeating ingredient across the thickness of a substrate (e.g., skin)
  - and the rate or kinetics of permeation

## Diffusion kinetics

- Fick's first law:

$$J = -D \frac{\partial C}{\partial x}$$

$C$  is the concentration and

$D$  is the diffusion coefficient

- Fick's second law:

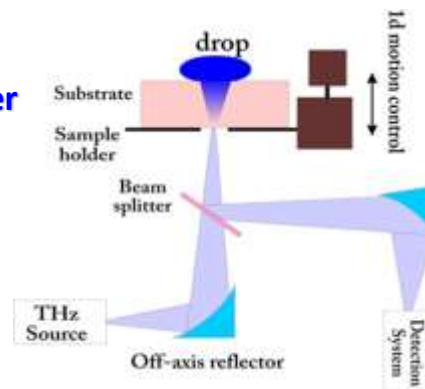
$$\partial C / \partial t = D \frac{\partial^2 C}{\partial x^2}$$

## Objective

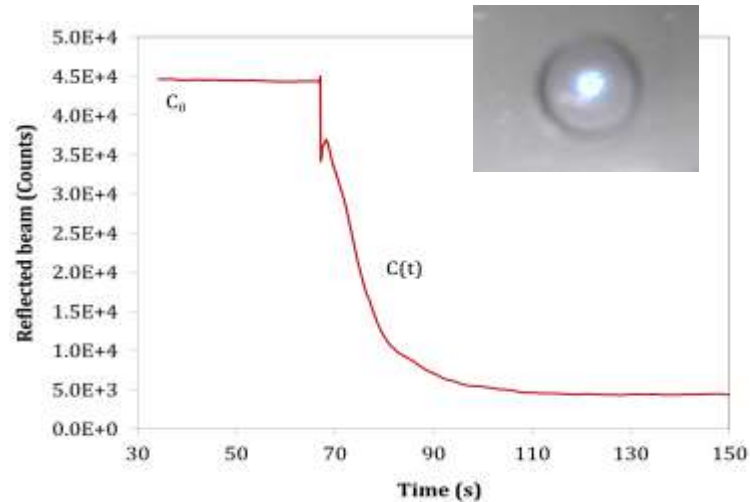
- To quantify the bioavailability of nanoparticles
- Quantify the kinetics and concentration gradient of actives in stratum corneum

## Experimental

- A CW terahertz is generated from electro-optic dendrimer
- Initially the terahertz beam remains focused on the substrate surface.
- A drop is applied and the kinetics is recorded in real-time  $\rightarrow \partial C / \partial t$
- The saturated substrate is then scanned  $\rightarrow \partial C / \partial x$

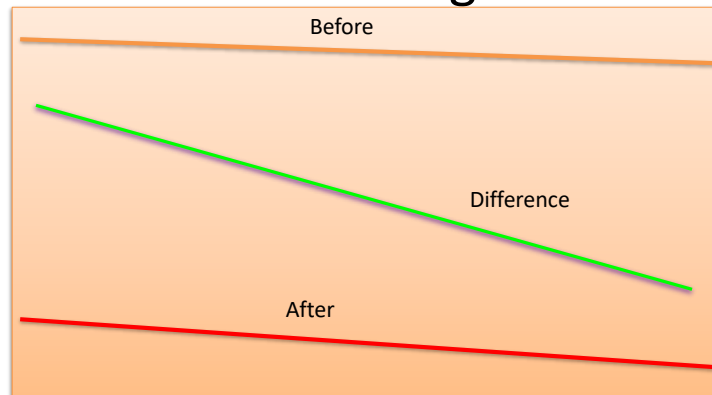


## Permeation Kinetics



Example: Permeation kinetics of DI water in glossy paper

## Concentration gradient

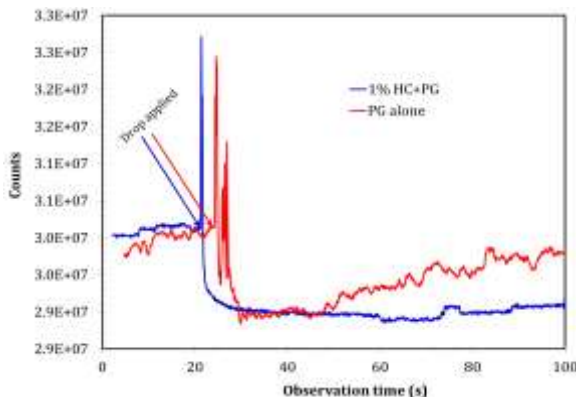


$$\left| \frac{\partial c}{\partial x} \right|_{Analyte} = \left| \frac{\partial c}{\partial x} \right|_{Before} - \left| \frac{\partial c}{\partial x} \right|_{After}$$

## Propylene glycol and caffeine

- Many formulations used in transdermal and topical drug delivery use water and/or propylene glycol as solvents or penetration enhancers.
- we examine permeation of two common compounds in the stratum corneum: (i) hydrocortisone dissolved in propylene glycol (PG), and (ii) caffeine dissolved in water.

## Kinetics of hydrocortisone penetration



Stratum Corneum mounted on the sample holder

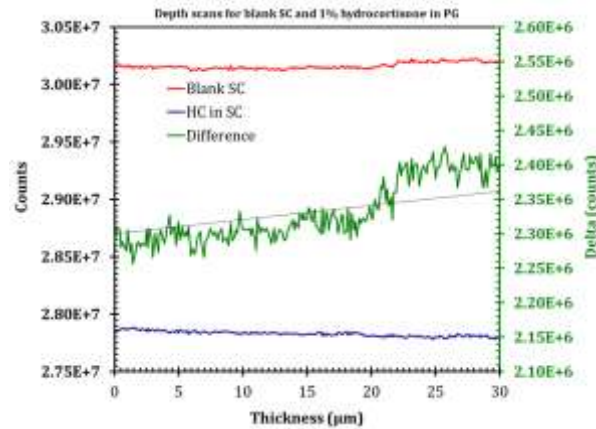
Kinetics of permeation of two solutions in to stratum corneum:

Red: Propylene glycol

Blue: 1% hydrocortisone in propylene glycol

Ref: Anis Rahman, Scott Frenchek, Brian Kilfoyle, Lina Petterkin, Aunik Rahman and Bozena Michniak-Kohn, "Diffusion Kinetics & Permeation Concentration of Human Stratum Corneum Characterization by Terahertz Scanning Reflectometry," *Drug Dev. Deliv.*, vol. 12, No. 4, May 2012, pp. 43-49.

## Concentration gradient of Hydrocortisone

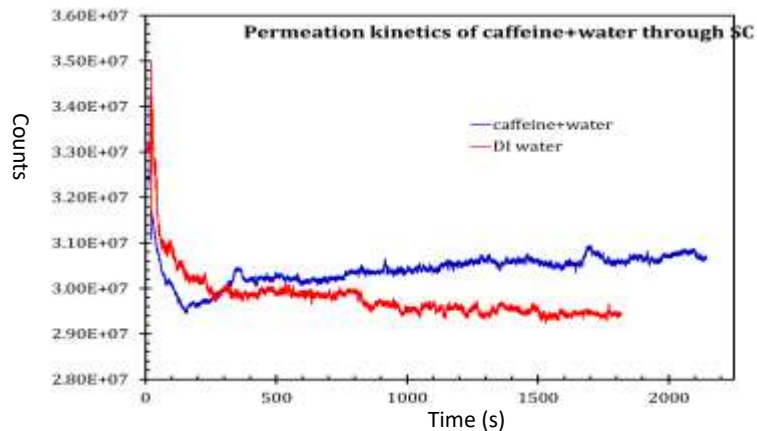


Ref: Anis Rahman, Scott Frenchek, Brian Kilfoyle, Lina Petterkin, Aunik Rahman and Bozena Michniak-Kohn, "Diffusion Kinetics & Permeation Concentration of Human Stratum Corneum Characterization by Terahertz Scanning Reflectometry," *Drug Dev. Deliv.*, vol. 12, No. 4, May 2012, pp. 43-49.



<http://arphotronics.net>  
(C) 2018 Anis Rahman

## Kinetics of caffeine penetration

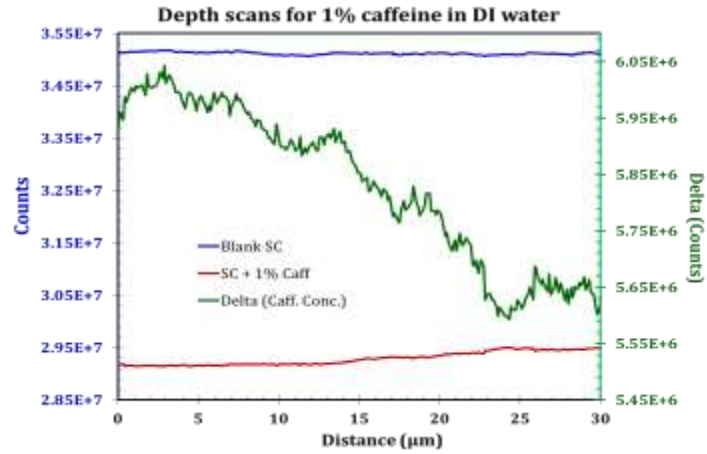


Ref: Anis Rahman, Scott Frenchek, Brian Kilfoyle, Lina Petterkin, Aunik Rahman and Bozena Michniak-Kohn, "Diffusion Kinetics & Permeation Concentration of Human Stratum Corneum Characterization by Terahertz Scanning Reflectometry," *Drug Dev. Deliv.*, vol. 12, No. 4, May 2012, pp. 43-49.



<http://arphotronics.net>  
(C) 2018 Anis Rahman

## Concentration gradient of caffeine

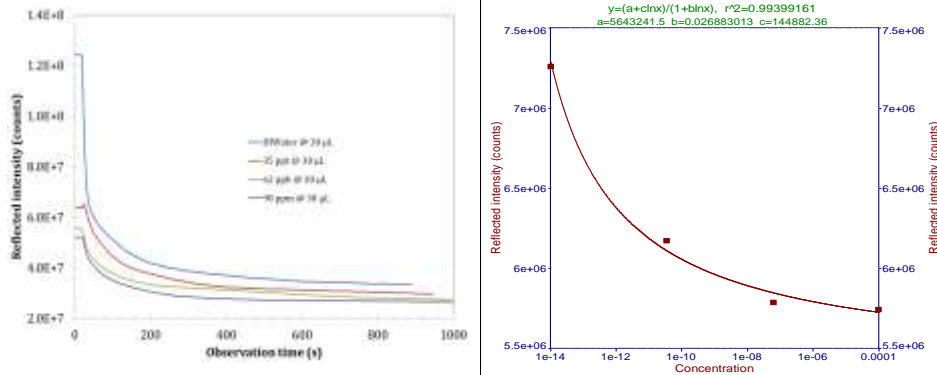


Ref: Anis Rahman, Scott Frenchek, Brian Kilfoyle, Lina Petterkin, Aunik Rahman and Bozena Michniak-Kohn, "Diffusion Kinetics & Permeation Concentration of Human Stratum Corneum Characterization by Terahertz Scanning Reflectometry," *Drug Dev. Deliv.*, vol. 12, No. 4, May 2012, pp. 43-49.



<http://arphotonics.net>  
(C) 2018 Anis Rahman

## Concentration dependence



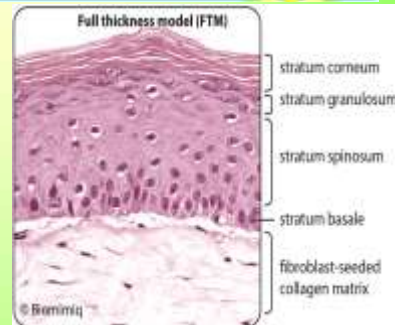
## Permeation of glycolic acid in to vitroskin



<http://arphotonics.net>  
(C) 2018 Anis Rahman

## Dermal fibroblasts

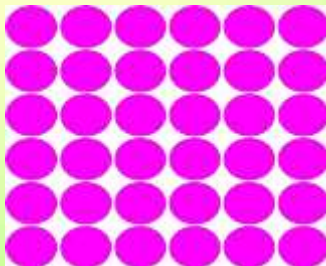
- An example of cultured skin cells for their interaction with nanoparticle
- Sample 1: Human skin cells, in particular, the dermal fibroblasts alone
- Sample 2: the same treated with titanium nano-particles
- The thickness profiling allows quantifying Ti nano-particles per fibroblast cell.



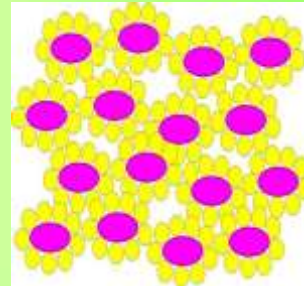
Ref: Anis Rahman, Tatsiana Mironava, Aunik Rahman, Miriam Rafailovich, "Terahertz scanning investigations of human dermal cells," in CLEO: Applications and Technology 2014, San Jose, California, United States, 8–13 June 2014, Paper No. AW3L.6, DOI: 10.1364/CLEO\_AT.2014.AW3L.6, ISBN: 978-1-55752-999-2

(C) 2018 Anis Rahman

## Rationale



Cultured fibroblasts cells



Cultured fibroblasts cells treated with Ti nanoparticles.

- Ti nanoparticles may be outside the cells or may penetrate inside the cells
- The thickness profile will be distinguishable for both cases

(C) 2018 Anis Rahman

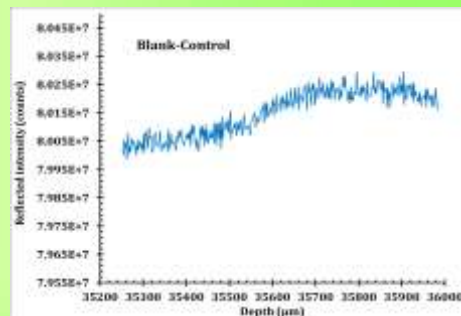
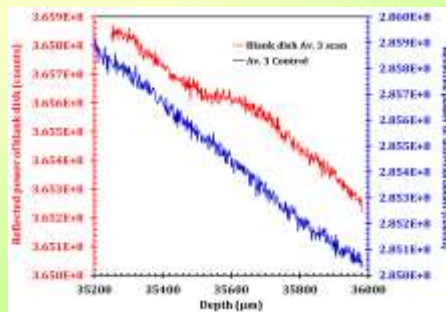
## Fibroblast scanning

- Petri dish is mounted on a Plexiglas fixture
- An opening in the bottom of the fixture allows exposing the samples to the T-rays.
- First, a blank petri dish is scanned across its thickness.
- This is used as the reference for all subsequent measurements



(C) 2018 Anis Rahman

## Profiles



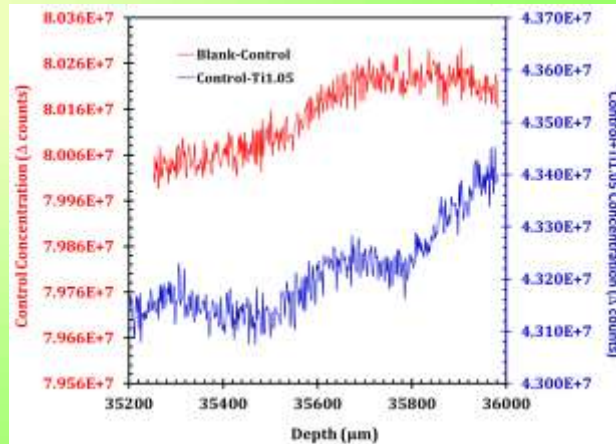
- Intensity profile of blank dish (red) and dish + fibroblasts (blue) across the thickness.
- Intensity decreased for the fibroblasts
- Thickness profile of the fibroblasts.
- To be compared with the intensity profile for the fibroblasts + Ti nanoparticles

(C) 2018 Anis Rahman

## Profile (distribution)

**Red:** Thickness profile of fibroblast cells (right Y-axis)

**Blue:** Thickness profile of fibroblasts treated with Ti nanoparticles



**Microscope is not able to see the differences**

Ref: Anis Rahman, Tatsiana Mironava, Aunik Rahman, Miriam Rafailovich, "Terahertz scanning investigations of human dermal cells," in CLEO: Applications and Technology 2014, San Jose, California, United States, 8–13 June 2014. Paper No. AW3L.6, DOI: 10.1364/CLEO\_AT.2014.AW3L.6. ISBN: 978-1-55752-999-2

(C) 2018 Anis Rahman

## Summary

- Terahertz scanning reflectometer has been used for quantitative measurement of layers in human skin and ti-nanoparticle coated fibroblasts
- A model is used for quantitative thickness profile of the dermal cells.
- Experiments will be conducted with varied concentrations of the nanoparticles.
- Number of nano-particle per fibroblast will be estimated from the calibration of the thickness profiles as a function of concentration

(C) 2018 Anis Rahman

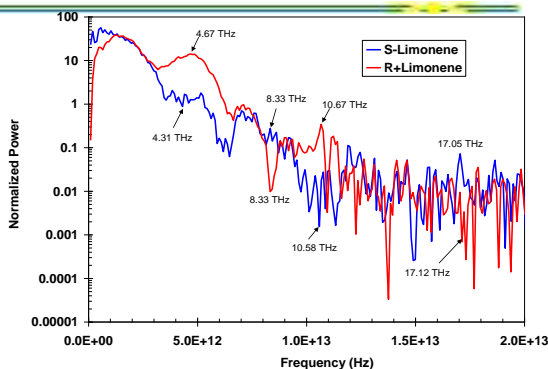
## Conclusions

- **Integrated Terahertz nanoscanning spectrometer is a unique tool for nano scale characterizations**
  - High sensitivity spectral characterization on 3D space
  - Non-destructive, Non-contact, sub-surface
  - Inspect 2D and 3D materials
  - Lattice defects, stacking faults
  - Defects, cracks, non-uniformity, inclusion, phases, etc.
- **All non-metals: Semiconductors, laminates, etc.**
- **May be extended to medical imaging/tomography**
- **Both quantitative measurement and visual inspection**
- **Collaboration available and interested.**

(C) 2018 Anis Rahman

## Molecular Chirality

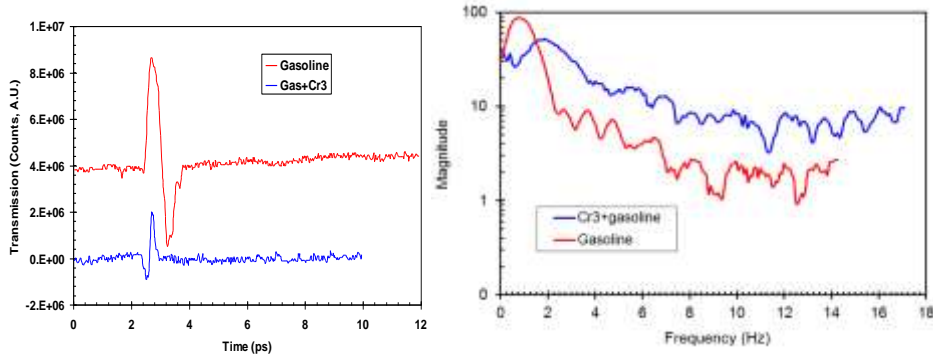
- **Visible light** stimulates electronic transitions that are symmetric (no net CD signal).
- These transitions respond equally to left and right circular polarizations.
- **THz radiation** tends to excite overall vibrational modes.
- Dynamic modes of oscillation respond differently to left versus right circular polarizations.
- **The spectra (right)** shows multiple chiral centers in the S-Limonene and R-Limonene molecules by opposing peaks at selected frequencies.



Samples courtesy of M Schramm, UC Long Beach

Ref: Michael P Schramm and Anis Rahman, "Label-free and neat detection of molecular chirality by terahertz spectrometry," Paper No. 36, 242<sup>nd</sup> ACS National Meeting, Wednesday, August 31, 2011, Colorado Convention Center, CO, USA

# Detecting contaminant in fuel



*Normalized time-resolved spectra of gasoline (red) and  $[(\text{CH}_3\text{CO}_2)_7\text{Cr}_3(\text{OH})_2]$  solution in gasoline at 1.91 mg/ml (blue). Presence of salt in gasoline reduces the transmission of THz power.*

*Fourier spectra of gasoline (red) and Cr3 solution (blue) corresponding to the time-resolved spectra (left). The spectra are clearly different for the two samples.*

(C) 2018 Anis Rahman

109

**Thank you for attending**  
**Questions are welcome**  
**Contact:**

**Anis Rahman PhD**  
**Applied Research & Photonics**

[info@arphotonics.net](mailto:info@arphotonics.net)

+1-717-623-8201

<http://arphotonics.net>

(C) 2018 Anis Rahman